Determining Flame Height And Flame Pulsation Frequency And Estimating Heat Release Rate From 3D Flame Reconstruction

by

Blair J. Stratton

Supervised by

Michael Spearpoint and

Charley Fleischmann

Fire Engineering Research Report 05/2

July 2005

A thesis submitted in partial fulfilment of the requirements for the degree of Master of Engineering in Fire Engineering

Department of Civil Engineering
University of Canterbury
Private Bag 4800
Christchurch, New Zealand

For a full list of reports please visit http://www.civil.canterbury.ac.nz/fire/fe_resrch_reps.shtml

Abstract

A method of creating a 3-dimensional point cloud representation of a buoyant diffusion flame from video footage from multiple angles has been created. This point cloud contains probabilities that the flame existed over the period the method was applied. This thesis uses these methods to determine flame height, flame pulsation frequency and flame volume from video footage of two furniture fires and one pool fire.

The flame height of the furniture and pool fires is compared to flame height predictions based on the heat release rate and estimated flame base diameter. The determined 'continuous' and 'intermittent' flame regions for the pool fire were always below the levels suggested by one of the predicting methods.

The flame pulsation frequency was compared to a widely used correlation based on the base diameter. This equation under-predicted the pulsation frequency grossly for the furniture fires and slightly for the pool fire. It was found that by increasing the period over which the pulsation frequency was determined pulsation frequency was lowered.

The flame volume was determined by summing the number of points in the point cloud representation and multiplying by the volume represented by each point. The flame volumes were compared to the experimental heat release rate from furniture calorimetry measurements to give an approximate correlation between the flame volume and the heat release rate. The values given by the method are in the same order of magnitude as given by other researchers, however insufficient video footage has been analysed to confirm the accuracy of the method.

It was hoped that the methods presented could be applied to fires outside of the laboratory, however attempts to use the methods presented here on video footage of a house fire were unsuccessful due to the poor quality of the footage taken.

Acknowledgements

I wish to thank my wife, Karyn. God only knows what I'd be without you.

Many thanks to my supervisors, Mike Spearpoint and Charley Fleischmann who provided invaluable insights, encouragement and precious time to my project.

Paul Mason introduced me to some of the tricks of using LabVIEW. His thesis was a very useful introduction to image manipulation and the theory behind videography, and his programs were adapted for use in this thesis.

Thanks to the New Zealand Fire Service Commission for providing me with a scholarship and for helping to fund the Fire Engineering program at Canterbury.

Thanks to my classmates who set a high standard and great work ethic over the last 24 months. It was a pleasure working with you all and I'm sure our paths will cross again in the real world.

Blair J. Stratton, 2005

Contents

List of Tables

List of Figures

List of Symbols

a	gradient fitted using LINEST in Excel	[-]
b	y-intercept fitted using LINEST in Excel	[-]
A_f	Flame Base Area	[m^2]

D	Flame Diameter	[m]
I	Flame Intermittency	[-]
L_m	Mean Flame Height	[m]
h_f	Flame Height	[m]
$\dot{Q}$	Rate of Heat Release	[kW]
Q*	Dimensionless Energy Release Rate	[-]
b	Plume Radius at Height, z (m)	[m]
z	Height	[m]
ΔT	Temperature Difference	[°C, K]
g	Acceleration due to Gravity	[=9.81 ms^{-2}]
c_p	Specific Heat Capacity at Constant Pressure	[kJ kg^{-1} K^{-1}]
$\dot{m}_p$	Plume Mass Flow at Height z (m)	[kg s^{-1}]
f	Flame Pulsation Frequency	[Hz]
ΔH_c	Heat of Combustion	[kJ kg^{-1}]
$\dot{m}''$	Free Burn Mass Loss Rate	[kg m^{-2} s^{-1}]
$\dot{m}''_\infty$	Free Burn Mass Loss Rate at Large Diameter	[kg m^{-2} s^{-1}]
M	Transformation Matrix	[-]
N	Number of Points in Point Cloud Grid	[-]
n	Normal Vector in Image Coordinate System	[m]
C	Pulsation Frequency Constant	[-]
C	Camera Position	[m]

R	Matrix Describing Image Rotation	[-]
T	Matrix Describing Image Translation	[-]
U	Flame velocity	[m s^{-1}]
u	Vector cross product of **n**x**v**	[m]
V	Flame Volume	[m^3]
v	Up Vector in Image Coordinate System	[m]
VRP	View Reference Point	[m]
x	Independent Variable	[-]
X	Bounds of Point Cloud in x-Direction	[m]
y	Dependant Variable	[-]
Y	Bounds of Point Cloud in y-Direction	[m]
Z	Bounds of Point Cloud in z-Direction	[m]

Greek Symbols

α	Constant in Flame Pulsation Frequency Equation	[-]
ρ	Density	[kg m^{-3}]
γ	Constant in Volume to Heat Release Rate Equation	[kW m^{-3}]
κ	Constant in McCaffrey Plume Equation	[m^a kW^b s^c]
χ	Combustion Efficiency	[-]
ν_e	Flame tip velocity	[m s^{-1}]
kβ	Fuel-Dependant Constant	[m^{-1}]
η	Constant in McCaffrey Plume Equation	[-]

Subscripts

∞	Ambient Conditions
max	Upper bound of grid
min	Lower bound of grid
x	x-direction
y	y-direction
z	z-direction
combined	Final transformation matrix
scale	Scaling Matrix
0	Value at 0% probability
25	Value at 25% probability
50	Value at 50% probability
75	Value at 75% probability

Chapter 1

Introduction

1.1 Motivation

There are a number of tools available for cataloguing the burning properties of a material or composite specimen (eg a piece of timber or an item of upholstered furniture), such as the cone calorimeter and ignitability apparatus, or the furniture calorimeter. Useful scientific data which can be measured using these various apparatus include the Energy Release Rate or Heat Release Rate (HRR), the time to ignition of a sample at a particular incident heat flux, as well as concentrations of gaseous products of the combustion reaction as the experiments are carried out. However useful they are, most of these techniques are unavailable to fire researchers when unwanted fire breaks out; indeed the only tool available at an unwanted fire scenario may be a video camera. The heat release rate cannot, at present, be estimated from video images. Conversely, other properties of the flame such as flame height and flame pulsation frequency can only be measured accurately using sophisticated video equipment.

1.2 Introduction

This thesis describes a method of converting video footage of typical fires (eg pool fires or upholstered furniture fires) into a time-averaged 3-dimensional representation of a flame. The method described involves a number of computational operations on multiple video images of fires. These operations include extracting a colour plane (eg 'blue') from each image, and thresholding the resulting image to locate regions containing the flame, and regions that do not. Following image manipulation, the flame images taken from several camera positions are translated through a point cloud, leaving behind a 3-dimensional representation of the flame. In this thesis, the representation of the flame is analysed further to determine properties of the flame including flame height and flame pulsation frequency, and flame volume. An attempt is made to find a correlation between the flame volume and the heat release rate of the fire, as well as to determine the flame height and flame pulsation frequency.

This thesis is presented as a 'proof of concept', and does not purport to contain an exhaustive analysis of the flame height, flame pulsation frequency, or flame volume of pool or furniture fires. Insufficient video footage was analysed to gain an accurate understanding of the

relation between video imagery and flame properties, however, an encouraging trend has been found between the properties of the 3-dimensional flame representation obtained from analysing video footage herein and expected values of these properties from literature correlations.

1.2.1 Hypothesis

It should be possible, using Mason's methods, to locate the flame tip in each of a series of projected images. The height of this point above the base of the fire is the flame height. Using common correlations for determining the flame height based on the heat release rate ($\dot{Q}$) and flame base diameter (D), the flame height can be estimated throughout the experiment. The accuracy of this method should therefore be reflected by how well the predicted flame height follows the determined flame height.

Flame pulsation frequency is generally estimated from empirical correlations derived from analysis of experimental flame height. Cox (1995), and Malalasekera (1996) both propose correlations in the form of Equation (1):

$$f = \frac{\alpha}{\sqrt{D}} \tag{1}$$

As the experimental flame height is determined from video footage for this thesis, it is therefore possible to determine the flame pulsation frequency for these experiments and compare to values obtained using Equation (1). As we are comparing similar methods for determining the flame pulsation frequency, if our height measurement is accurate, then it should compare to the results from applying Equation (1).

It is thought that there exists a correlation between the heat release rate ($\dot{Q}$) and the volume of a flame on the order of approximately 500 kW m^{-3} (Cox, 1995), however there are few methods available for accurately determining the flame volume which can be used in order to test this hypothesis. Mason (2003) showed in his thesis that it is possible to manipulate video images of buoyant diffusion flames (specifically pool and furniture fires) into 3-dimensional representations of the flame. Mason's method is one of few methods available which can be used for determining the flame volume, which can be further compared to the heat release rate of the fire in order to determine whether any correlation exists between the two properties. Another method available for determining the heat release rate relies on an assumed flame

shape (which comprises a cone sitting atop a cylinder two thirds of the measured or estimated flame height) (Audouin, 1995).

1.2.2 Aim

The aim of this thesis is to determine flame properties such as height and volume from a 3-dimensional representation of the flame obtained using Mason's methods. These properties, respectively, are further analysed to determine the flame pulsation frequency, and to ascertain whether a correlation exists between the heat release rate and flame volume. The flame height obtained using the methods described in this thesis is compared to the flame height determined using literature correlations, which are generally based on the flame base diameter and heat release rate.

The flame height is also used to determine the flame volume and hence the heat release rate using Audouin's cone and cylinder method mentioned above, which allows comparison between this method and the method described herein for determining the heat release rate from flame volume.

1.3 Thesis Overview

Chapter 2 – Background Information and Literature Review: This chapter presents a review of literature on video and image processing, flame height and pulsation frequency determination, and methods available for calculating heat release rate from experimental measurements and empirical correlations.

Chapter 3 – Processing Video Footage Using the Minima Reconstruction Technique (MRT): Much of the work presented in this thesis builds on that of Mason, who developed a computational method of creating a 3-dimensional point cloud by 'averaging' video images of fires which were taken from several directions and projecting the images through a 3 dimensional field. His work was intended for the purpose of determining the radiative heat flux at distances away from the flame. Mason's programs are developed further in this thesis to determine whether it is possible to glean heat release rate and flame height information from video footage using his techniques. Chapter 3 outlines the methods developed by Mason and introduces the modifications made to his programs for this study, to be further developed in the relevant chapters.

Chapter 4 – Flame Height: The MRT method is used to determine the flame height during two furniture fires and one pool fire. A small sample of these results is compared to the video footage to see whether the technique is accurate. The determined flame heights are compared to well known correlations, which estimate flame height based on the diameter of the base of the flame and the magnitude of the heat release rate. The applicability of these correlations to furniture fires and the success of the methods described herein to determine flame height will be presented.

Chapter 5 – Flame Pulsation Frequency: Pulsation frequency for buoyant diffusion flames has been described by simple equations based solely on the base diameter of the flame. From the literature reviewed, it is unclear whether this correlation was derived from pool fires, however it seems to under-predict the flame pulsation frequency of furniture fires.

Chapter 6 – Flame Volume Measurement: Knowing the flame volume is not particularly useful information to a fire engineer/researcher presently, however it is thought that the flame volume is at least an approximate indication of the amount of heat being given off the flame. This chapter describes a method for accurately determining flame volume and compares furniture fire flame volumes to the experimental heat release rate. An attempt is therefore made to investigate the existence of a correlation between the flame volume and heat release rate for upholstered furniture fires. This correlation is then applied to a methanol pool fire, video footage of which undergoes the minima reduction technique.

Appendix A contains information about the chairs which were burnt and from which video footage was analysed in this thesis.

Appendix B contains an overview of the LabVIEW programs written for this thesis.

Chapter 2

Background Information and Literature Review

2.1 Introduction

The literature reviewed for this thesis generally fits into one or more of four key areas: how to capture and process video images of flames, flame height, flame pulsation frequency and flame volume.

2.2 Photographic and Video Image Manipulation

This thesis extends the work done by Mason (2003) which will be covered in more detail in Chapter 3. He presented a method of converting video footage of flames into a 3-dimensional representation of a flame. A surface fitted to the point cloud he developed was used to estimate the radiation being emitted from the surface. This surface was fitted using a radial basis function. This procedure is described in more detail in Chapter 3.

Generally, previous methods for determining flame characteristics from film or photographic images have not used digital image processing techniques, and have relied on the researcher performing tedious measurements on the actual photographic or cine-film. This was due largely to the expense of digital cameras, and the lack of computer processing power available.

Laskey and co-workers (1984) determined flame height by visual observation, photographic studies and high speed cinematography. They did not use computers to examine their data, the fastest of which would have had insufficient processing power at the time their work was performed.

Flame luminosity was mapped using a video camera by Coutin and co-workers (1999). This was done to enable wall flame heights to be measured and allowed them to develop new wall flame height correlations to include the effects of burner height, wall width and sidewall confinement.

2.3 Flame Height

Predicting the height of the flame above the burning object enables a fire engineer to calculate the temperature of the plume/ceiling jet at various points above the fire. Experimental flame height is generally measured during experiments by examining a series of still, high speed photographs by eye or using a computational method. Non-photographical techniques exist however, such as that proposed by Simard and co-workers (1989), who hung lengths of solder in an array which melted as the moving flame front passed by. The remaining solder gave a reasonably accurate indication of the maximum height reached by the flame at each position in the array (the accuracy of this method largely depends on the composition of the solder used).

Numerous correlations have been derived to predict flame height in design fire scenarios for various purposes, including the design of effective fire safety systems such as sprinkler systems.

The flame height can be estimated using correlations such as those given by McCaffrey (1995), Zukoski (1984) or Heskestad (2002), which all require the heat release rate of the fire, $\dot{Q}$, to be known, while the Zukoski and Heskestad plumes require the characteristic dimension, D, to be given. D is usually the diameter of the base of the flame. Another common correlation, attributed to Thomas et al. (1963) will not be used here due to its limited applicability to fires with the diameter much greater than the flame height. The diameter of fires examined in this thesis is generally smaller than the height of the flame. As explained above the rate of heat release is difficult to obtain for some fires, which makes estimation of the flame height impossible using the non-photographic techniques currently available.

McCaffrey (1995) found plume relationships for upward velocity and temperature from experimental data and dimensional analysis. He divided the fire plume into three regions: the continuous, intermittent and plume regions. The location of each of these regions was based on the heat release rate, $\dot{Q}$. These correlations are given below:

$$\Delta T_0 = \left(\frac{\kappa}{0.9.\sqrt{2.g}} \right)^2 \left(\frac{z}{\dot{Q}^{2/5}} \right)^{2\eta-1} .T_\infty \tag{2}$$

$$u_0 = \kappa\left(\frac{z}{\dot{Q}^{2/5}}\right)^{\eta}\dot{Q}^{1/5} \tag{3}$$

The constants η and κ vary depending on the plume region:

Table 2-1 – Constants in McCaffrey's Plume Equations

Region	**$z/\dot{Q}^{2/5}$ [m kW$^{-2/5}$]**	**η**	**κ**
Continuous	<0.08	½	6.8 [m$^{1/2}$ s^{-1}]
Intermittent	0.08-0.2	0	1.9 [m kW$^{-1/5}$ s^{-1}]
Plume	>0.2	-1/3	1.1[m$^{4/4}$ kW$^{-1/3}$ s^{-1}]

The quotient $z/\dot{Q}^{2/5}$ can therefore be used to locate the boundaries of the continuous and intermittent plume regions. The continuous region should be comparable to the lowest flame height measured during experiments, and the intermittent region should be the area between this point and the uppermost flame height measurement.

While it will be attempted to compare the flame heights determined by the techniques proposed in this thesis to the predicted heights of McCaffrey's continuous and intermittent plume regions, the Zukoski plume will not be examined because the plume mass flow rate, $\dot{m}_p$, at height, z, was not measured and the equation does not specify the location of the flame tip. Heskestad's equation will be used for estimating mean flame heights based on the base diameter and the experimental heat release rate. For the upholstered furniture fire videos analysed, the base diameter was assumed to be 2 m, as accurate measurements of this dimension were not made. The experimental heat release rate was obtained from measurements taken by the furniture calorimeter at the University of Canterbury.

Flame height above pool fires can be estimated using one of a variety of plume correlations including the so-called ideal plume, however the application of this latter correlation to furniture fires is limited, especially when little experimental data, such as the heat release rate, plume centreline temperatures and mass flows is known.

2.3.1 Mean Flame Heights

Heskestad proposed the following equation for determining the mean flame height, L, for turbulent diffusion flames (but not jet flames) based on McCaffrey's (2002) work:

$$L = 0.235\dot{Q}^{2/5} - 1.02D \tag{4}$$

The energy release rate, $\dot{Q}$ is given in kW and the diameter, D, in m. Using an estimate for the flame diameter and given the instantaneous heat release rate as determined from furniture calorimeter measurements, this equation will be used to verify the flame heights measured using the techniques developed in this thesis.

The derivation of Equation (4) relies on the dimensionless energy release rate, Q*, which, according to Heskestad (1997), was in turn originally derived from non-reacting turbulent plumes and does not take into account the effect of ambient temperature [15]. A higher ambient temperature will generally result in a higher flame height than predicted by Equation (4), while a lower ambient temperature results in a lower flame height. However these effects only apply appreciably when ambient temperatures are approximately 40-50 °C above or below normal experimental conditions, so we will not concern ourselves further with this problem here.

2.3.2 The Ideal Plume

This description is given in Karlsson and Quintiere (2000). Most plume correlations are based in part on the ideal plume (sometimes called the 'point-source plume'), first presented by which assumes there is a point source of heat at height, z=0. The driving force in the system is due to density differences between the air above the point and the cold surrounding air. The following is assumed:

- All energy enters the system at the point source origin and remains in the plume.
- Density variations throughout the plume are small and for the most part it is assumed that the ambient density, ρ_∞, is equal to the plume density, ρ.
- The form of the velocity, temperature and force profiles are independent of the height, z. For the ideal plume these profiles are assumed constant within the plume radius and equal to the ambient conditions outside the plume (the so-called 'top hat' profile.)

- The air entrainment at the edge of the plume (the horizontal entrainment velocity) is assumed to be 15% of the upward gas velocity in the plume.

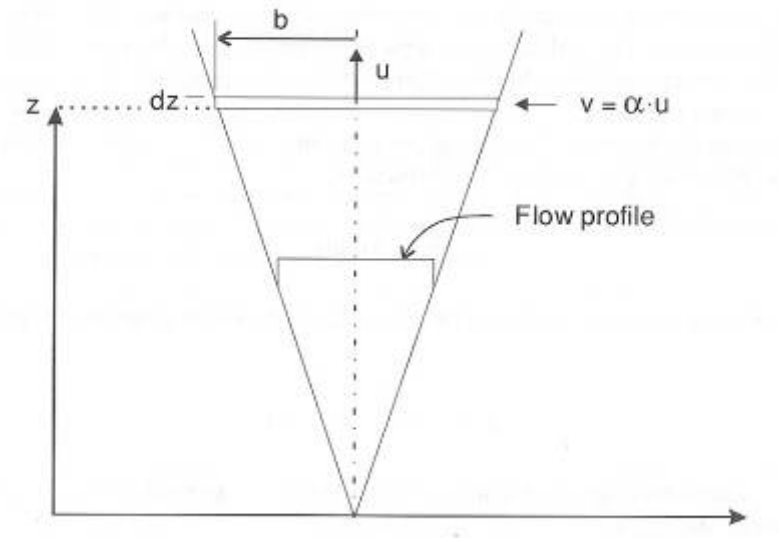

Figure 2-1 – Ideal Plume Representation (taken from Karlsson and Quintiere (2000)).

The derivation of the following equations for the ideal plume can also be found in Karlsson and Quintiere (2000).

Plume Radius at height z:

$$b = 0.18z \tag{5}$$

Temperature difference at height z:

$$\Delta T = 5.0\left(\frac{T_\infty}{g c_p^2 \rho_\infty^2}\right)^{1/3} \dot{Q}^{1/3} z^{-5/3} \tag{6}$$

Upward gas velocity at height z:

$$u = 1.94\left[\frac{g}{c_p T_\infty \rho_\infty}\right]^{1/3} \dot{Q}^{1/3} z^{-1/3} \tag{7}$$

Plume mass flow at height z:

$$\dot{m}_p = 0.20\left(\frac{\rho_\infty^2 g}{c_p T_\infty}\right)^{1/3} \dot{Q}^{1/3} z^{-5/3} \tag{8}$$

The equations above are unsuitable for accurately predicting the flame height of a furniture fire. Too many unknowns are present in the equations when the only information available is the size and position of the flame as given by the video footage. Neither the plume mass flow nor the centreline velocity was measured during the furniture fire experiments. Although the centreline plume temperature was measured, the absence of too many experimental measurements make the above correlations unusable for comparing the predicted flame height to that determined using our methods. Simpler correlations such as McCaffrey's (Equations (2), (3)) or Heskestad's (Equation (4)) will be used for this work.

The mean flame height has been defined by Zukoski and co-workers (1984) in terms of the intermittency of the flame, I [-]. The intermittency is defined as the fraction of time that part of the flame is above a certain height, z [m]. The mean flame height is then the height at which the intermittency is 0.5. A typical graph of intermittency vs flame height is given as Figure 2-2 below.

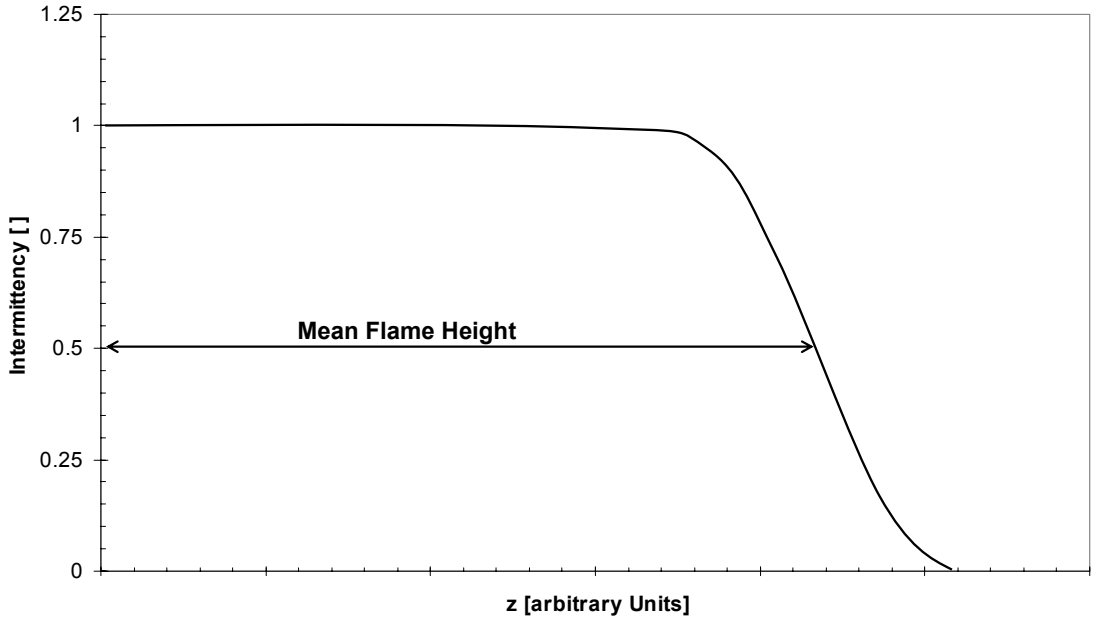

Figure 2-2 - Mean Flame Height as Defined by Zukoski et al. as a Function of Flame Intermittency

Audouin and co-workers (1995) performed a similar technique to that described by Mason and defined the continuous and intermittent flame heights as the distance above the burner where the flame probability was more than 0.95 and less than 0.05, respectively. For determining flame height in this thesis we will investigate individual frames of flame footage, which will be thresholded into regions containing the flame, and regions not containing the

flame. For each individual frame, therefore, there are only two levels of flame probability – 0% or 100% and the method of Audouin will not apply in this case. A 2 dimensional field of average probabilities of flame position can be obtained by 'averaging' several seconds of thresholded images. This technique is further explained in Chapter 3 and is used in this thesis for determining the average flame volume over 6 seconds of footage.

2.4 Flame Pulsation Frequency

A typical flame will be observed to have a non-constant height of combustion. Eddy/vortex shedding and a recently proposed theory of inviscid flow "buckling" (whereby flame tips stretch and collapse) are explanations for flame pulsation ((Puri, 1993). Barr (1952) described the process as "a progressive necking which eventually led to flame separation. The upper flame bubble would burn itself out, while the lower, anchored portion continued to grow in length". This necking can occur at the tip of the flame or at the side of the flame, which leads to difficulties in creating automated methods of measuring the flame pulsation frequency.

Typical flame pulsation frequencies including those given off by furniture fires have been reported by Cox (1995) to lie between from 0.4 to 10 Hz. Early work by Chamberlin and Rose (1928) and later by Barr (1952) gave results on the order of 10 and 8 Hz, respectively. Cox states that a candle or similar laminar diffusion flame will have a pulsation frequency of close to 11 Hz, with pulsation frequency decreasing as the base diameter of the flame increases.

The pulsation frequency is measured by some InfraRed (IR) flame detection equipment. According to Roberts (2003), IR flame detectors "comprise a filter and lens system used to filter out unwanted wavelengths and focus those remaining on a photovoltaic or photoresistive cell sensitive to IR energy. They can respond just to the resulting net IR component of the flame or in combination with a flame [pulsation frequency] sensor (typically looking for a [pulsation frequency] rate of 5 to 30 Hz.)" It is obviously necessary that signals from unwanted fires being measured by such detection equipment are not interpreted as a 'safe' source, say a candle. It is important then to know the range of pulsation frequencies to be expected from a range of potential fire sources, such as furniture fires, pool fires or welding equipment.

Bhaduri (1968) found that the frequency and amplitude of the pulsing flame depend on the "fuel-air ratio, initial temperature of the mixture and linear dimension of the combustion chamber…" However a common correlation found for estimating flame pulsation frequency depends only on the flame diameter:

$$f = \frac{\alpha}{\sqrt{D}} \tag{9}$$

This correlation was given by Cox (1995) with a constant $\alpha = 1.5$ and Malalasekera and co-workers (1996) gave $\alpha = 1.68$. For a flame with diameter D = 0.8 m, the pulsation frequency is estimated as f = 1.7-1.9 Hz. The results of these correlations appear to underestimate the flame pulsation frequency for upholstered furniture fires, however the general trend that the pulsation frequency should decrease with increasing flame base diameter seems correct from observation. A slightly more complex correlation than Equation (1) was derived by Puri (1993) for semi infinite horizontal solids:

$$f = \frac{0.2045\left(g^{0.6} / \nu_e^{-0.2}\right)}{\left(CD/2\right)^{0.8}} \tag{10}$$

Here C is a constant that must be found empirically and ν_e is the flame velocity. Neither of these values was obtained along with the flame footage examined in this thesis so this correlation is not used here.

Malalasekera and co-workers (1996) reviewed experimental techniques for flow visualisation (the results of which can then be used to describe the flame pulsation frequency as well as flame height) including:

- Temperature measurement – small, robust thermocouples are inserted into the flame. The technique requires the thermal inertia of the instruments to be compensated for to gain the instantaneous temperature value.

- Dynamic pressure measurement – a pitot probe is inserted into the flame to measure the local dynamic pressure, which is related to the flow velocity by the equation $P = 1/2\rho U^2$, where ρ is the flame gas density [kg m^{-3}] and U is the gas flow velocity [m s^{-1}].

- Laser-Doppler anemometry – a non-intrusive measurement technique that relies on seeding the fire source and oxidiser equally with tracer particles which describe the velocity.

- Static pressure measurement – The burner supply is tapped and the fluctuating static pressure in the fuel line is determined.

Since we are concentrating on video footage for this thesis, none of these techniques were investigated further in this thesis.

2.5 Flame Volume and Heat Release Rate

At present there is no accurate method of determining the volume of an uncontrolled buoyant diffusion flame at any instant in time. Such a flame occurs when upholstered furniture burns or during a pool fire, with the buoyant forces due to density differences between the plume and ambient gases being higher than the momentum forces from the flame source. It is thought, however, that there is a simple correlation between the flame volume and the heat release rate, which Cox (1995) proposed is on the order of 500 kW m^{-3}. Although this figure sounds like a reasonable estimate, Cox referred to a paper by Bradley (1992) for this value, where no such constant was to be found for turbulent diffusion flames.

Rasbash et. al. (2004) imply a similar relationship between the heat release rate and the flame volume, with the flame in this case being assumed to have a volume consisting of a cone on top of a cylinder roughly one half to two thirds of the height of the flame. The correlation is given by Rasbash for calculating the flame volume in terms of the heat release rate:

$$V = 1.21\dot{Q}^{1.18} \tag{11}$$

This can be rearranged as follows:

$$\ln V = \ln 1.21 + \ln \dot{Q}^{1.18}$$

$$\dot{Q} = \exp\left(\frac{\ln V - \ln 1.21}{1.18}\right)$$

$$\dot{Q} = \frac{\exp\left(\ln V^{1/1.18}\right)}{\exp\left(\ln 1.21^{1/1.18}\right)}$$

$$\dot{Q} = 0.851V^{0.847} \quad (10\text{ a})$$

The constants in this equation are of limited use due to the simple flame shape which was assumed for their derivation. Rasbash et. al. realise this as they note that "empirical information on mean flame shapes would be helpful."

Accurate measurement of the flame volume concurrently with the heat release rate may enable the development of such a correlation. Ergo, in fields of study where the heat release rate is unable to be measured using oxygen consumption calorimetry, the volume of the flame, as determined from video footage, should provide the basis of a reasonable estimate of the heat release rate of the fire. Such scenarios may include scrub or forest fires, vehicle or projecting flames from building fires: there is neither sufficient time nor large enough facilities available to perform measurements of the heat release rate.

A method to accurately describe the volume of a buoyant flame is described here using techniques first developed by Mason (2003). The existence of a correlation between flame volume and heat release rate will be investigated using this method. If it exists, such a correlation could be used to convert video footage of a real fire, say a forest/scrub fire, into a crude estimate of heat release rate. This is an ability fire researchers do not currently have.

2.5.1 Measurement of Heat Release Rate using the Furniture Calorimeter

The furniture calorimeter is a large scale apparatus capable of collecting gases given off from a sample during a fire experiment (NT FIRE 032, 1991). Oxygen consumption calorimetry is used to convert the gas concentrations recorded into a heat release rate for the sample [kW]. The principal behind oxygen consumption calorimetry is that the amount of oxygen consumed by a fire is directly proportional to the heat release rate of the fire (for most fuels it is assumed that 1 kg of oxygen consumed = 13.1 MW given off) (Huggett, 1980). By measuring the concentration of oxygen during the experiment and comparing it to the 'prebaseline' (pre-experimental) oxygen concentration measurement, the heat release rate can be found over the course of the experiment. By shooting video footage of a fire experiment while measuring the heat release rate, it should be possible to provide a correlation between the heat release rate and the flame volume.

Chapter 3

Processing Video Footage Using the Minima Reconstruction Technique (MRT)

3.1 Video Camera Use and File Storage

The digital video cameras which were used to capture the videos analysed in this thesis are JVC GR-DV 2000 cameras capable of taking 25 frames per second at 1.92 Mega Pixel resolution using progressive scan technology. Progressive Scan is an image sensing method which picks up all the lines of picture information in one scan, as opposed to regular shooting which records 'odd' and 'even' fields, resulting in a time lag between the fields. When the fields are combined to make one frame they may display a jittery image especially when recording a moving image. With progressive scan a calmer image is recorded.

Cameras capable of responding to infra-red or thermal radiation are expensive and were therefore not considered for use in this study. Further work may include their use in a flame intensity or location study.

When taking footage to be analysed, the zoom feature of the camera should be set at its widest setting (images seem far away) and must not be altered during filming. Zooming in makes it difficult to know the theoretical position of the camera lens in relation to the points in the screen during reconstruction. It would be theoretically possible to create a computer program to locate at least two distinct points at known positions and orientations and back-calculate this theoretical camera position based on their size and position in each frame, however this would require careful planning before the experiments, which is not always possible.

Due to the rectangular nature of the video image, turning the camera on its side is often required in order to capture the entire flame. This will require extra manipulation of the images (i.e. rotation.)

Mason suggests avoiding using any form of video compression to avoid 'blocky' images and loss of flame information. The video files analysed for this work were not compressed. This means that a large amount of data storage space must be available to perform these techniques. An uncompressed 5 minute '.avi' video takes up approximately 1 Gigabyte

(1 GigaByte, GB = 1,048,576 KiloBytes, KB) of disk space. Each frame in such a video takes up approximately 220-250 Kilobytes, so storing each frame in a 5 minute, 7500 frame video takes up a further 1.6-1.8 GB. Finally, converting every frame into a binary image can take a further 100 MB. It is therefore advisable to have approximately 5-10 GB free hard drive space when starting to analyse video files of fires. With the current increasing availability of 400+ GB capacity hard drives, this storage recommendation will soon be less relevant.

A video camera uses a Charge Coupled Device (or CCD, a semiconductor that is sensitive to light) to turn an image into a digital reading. Each pixel in a CCD such as that in a video camera can be considered to be a well of electrons. The image is formed due to light entering an array of electron 'wells' causing the wells to fill up with electrons. The amount of charge in each well is automatically converted to an intensity reading. Overexposure can occur if the amount of light entering each electron well is higher than the full well capacity. The brightness is limited by the camera's auto exposure function. This feature cannot be turned off with the video cameras used in this thesis. Overexposure can make an image seem more washed out and less sharp. However, allowing the exposure of the camera to change during the experiment means it is more difficult to compare the flame size/position in images early in the experiment (when the pixels are unsaturated due to the small flame size) to that later on (when the intense flame forces the camera to limit the exposure and the entire room seems to darken.) This can lead to 'holes' in the flame that must be filled in during image processing (see Section 3.2.5 below), lest they be interpreted as perforations in the flame sheet. There is little that can be done to prevent overexposure when recording flames on most 'consumer grade' video cameras but it is worth noting that it may cause the visible flame to be smaller than in reality especially later on in the experiment when the flame takes up more of the image. This should not impact greatly on the accuracy of the techniques presented here.

For the techniques used here, it is vital to know the position of the camera relative to two stationary points in each frame, so measurements relating the distance from the centre of the camera lens and these two points to an origin should be taken prior to the experiment. It is difficult to take such measurements during the experiment and reference points such as chair arms may have moved during the experiment.

3.2 Image Synchronisation and Manipulation

3.2.1 Synchronisation of Video Footage from Multiple Angles

When taking video footage from more than one direction, it is important to be able to synchronise the footage. Since we used identical cameras for this work each with a frame rate of 0.04 seconds, simply finding a frame containing an event such as the moment the fire is lit is sufficient to synchronise the two videos to within ±0.04 seconds. Mason suggests synchronising the videos by using a photographic flash unit to illuminate a single frame of each video if the frame rate is different in each camera. However such equipment will not always be available when taking footage of unwanted fires.

3.2.2 Image Manipulation

The following techniques were developed by Mason (2003) to extract a 3 dimensional cloud of points describing the flame from two or more video files of a fire. In his thesis Mason described how to convert still frames taken from video footage into averaged greyscale images. Multiple camera angles of a single fire are usually taken. For the furniture fires examined herein, two cameras exist at positions orthogonal to the fire as shown in Figure 3-1. The cameras do not have to be at 90° angles. If more than two camera angles are used, equal spacing around the object is suggested by Mason to reduce perspective error.

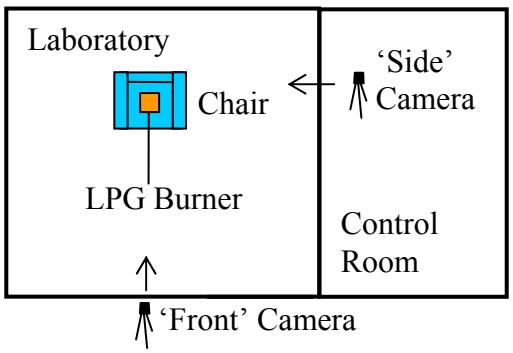

Figure 3-1 – Laboratory layout and description of camera positions

Freely available software can extract .jpg files of each frame from the video files. The .jpg picture format is chosen because it results in a small file (approximately 220 KB per frame for our purposes) without appreciable loss of picture quality. Each picture undergoes a series of operations.

3.2.3 Colour Plane Extraction

The object of this step is to extract a greyscale image with the most contrast between the flame and its background. A sharp distinction between the flame and the background is sometimes difficult to achieve and one must experiment to find the appropriate colour plane to extract for a given video file. Figure 3-2 shows the extraction of the blue colour plane from a colour image of a fire. Other colour planes available include:

Red	Hue
Blue	Saturation
Green	Luminance

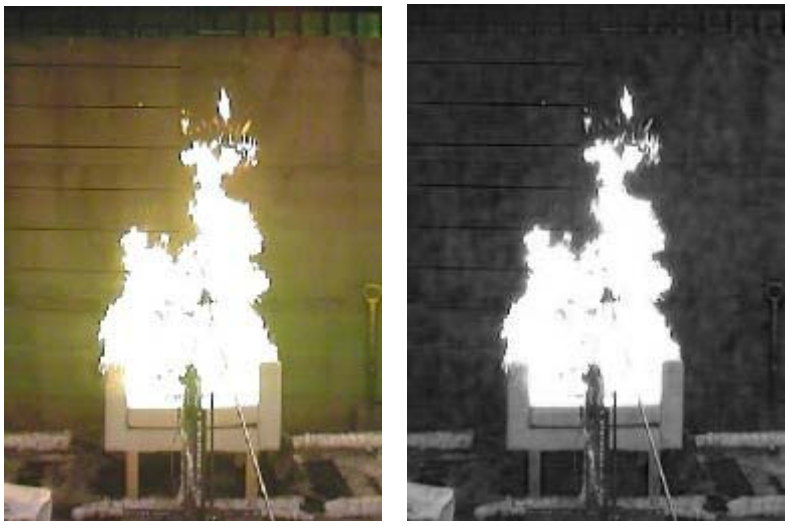

(a) **(b)**

Figure 3-2 – Extracting Blue Colour Plane from a Frame of Burning Item 'Chair 16'

3.2.4 Thresholding an Image

The image is converted from a greyscale image (with 256 intensity values, valued from 0-black to 255-white) to a binary image (with each pixel having a value of 0-black or 1-white.) Each point in the image is divided into one of two possibilities – that containing pixels above a certain greyscale value (i.e. the 'white' pixels containing the flame) and everything else. The image is set to black in those areas that do not contain the flame and the areas containing the flame are white. The upper value for thresholding is 255, while the lower value must be determined by experimentation for each video file individually, and lies at around 160.

Figure 3-3 shows the result of thresholding the image in Figure 3-2 (b) within the limits (160, 255).

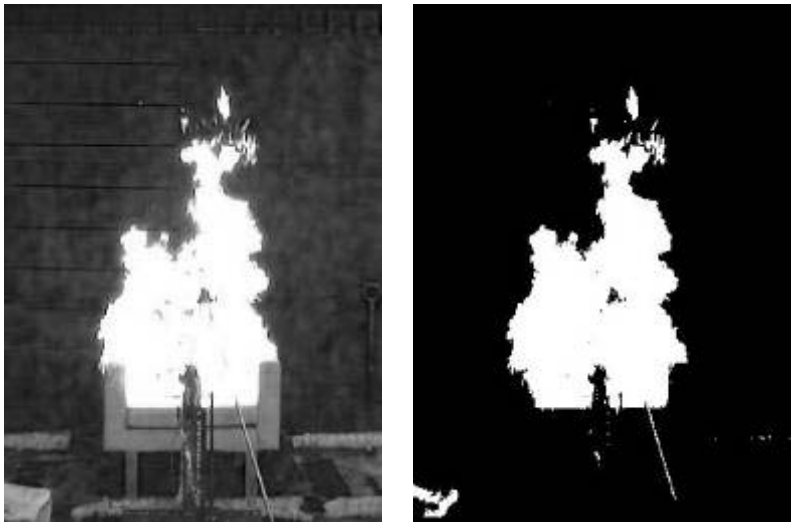

(a) **(b)**

Figure 3-3 – Thresholding a Greyscale Image

3.2.5 Filling Holes

The image required may contain holes due to the video being dark and failing to capture thin areas of flame. These holes would be interpreted as perforations in the flame sheet, when in fact they are an artefact of the auto exposure feature of the camera. This may become especially prevalent as the fire progresses and the exposure of the camera is limited to prevent overexposure (see Section 3.1.) A 'fill holes' algorithm can locate and improve the data quality of such areas within the flame (Ruether, 2002). Figure 3-4 shows the result of applying the fill-holes algorithm to Figure 3-3 (b)

Figure 3-4 – Filling Holes. The Section Inside the Circle in (a) is Part of the Flame that is Filled in by the 'Fill Holes' Algorithm.

3.2.6 Masking

Reflective surfaces in the camera's field of vision may leave an area with a high greyscale value which remains in the image after thresholding. It is sometimes possible to remove these areas without affecting the flame area. The area containing the flame can be selected using an image mask technique to discard image information outside the region of interest as in Figure 3-5.

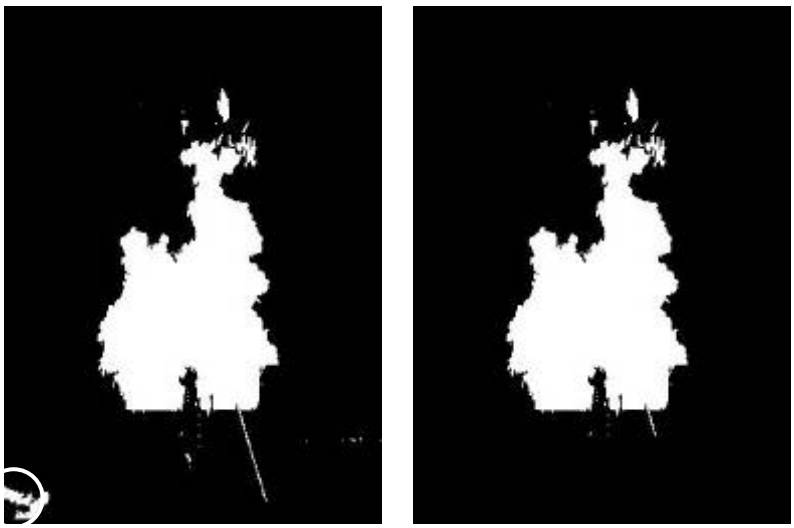

Figure 3-5 – Image masking. The Area Inside the Circle in the Bottom Left Corner is Part of the Image that is Removed Because it could not be a Part of the Flame

3.2.7 Image averaging

The binary images can be 'added' pixelwise, multiplied by 256 and divided by the number of images to create a new 8-bit image (again with 256 greyscale values.) For instance, if a pixel is white in one image and black in the next two, the averaged value for this location will be (1+0+0)*256/3 = a greyscale value of 85. Each greyscale value of the averaged image now relates to the probability of the flame existing at each point in the image, with the point just described having a probability of 33%. Points near the base of the flame exist in nearly every frame of the video, so these points are nearly white, with a greyscale value of nearly 255. This corresponds to a 100% probability that the flame exists at this point during the period the video was taken. Conversely, points where the flame never passed will have a greyscale value of 0 (black), with 0% probability that the flame existed at this point.

For the purposes of this thesis, for techniques involving determining the flame volume, 6 seconds of video images are averaged using this technique. For the flame pulsation frequency and flame height sections, only single frames are used, so this last step is unnecessary. For illustrative purposes, five frames in Figure 3-6 are manipulated as described in Sections 3.2.3 to 3.2.6 to produce Figure 3-7. The images are then 'added' to one another to create Figure 3-8. This requires a computer program to go through the images pixel by pixel and keeping a tally of the number of times that each pixel position is 'white' in the images. The final total for each pixel is multiplied by 255 to give a range of greyscale pixels from 0 (black) to 255 (white). The result is an 8-bit greyscale image.

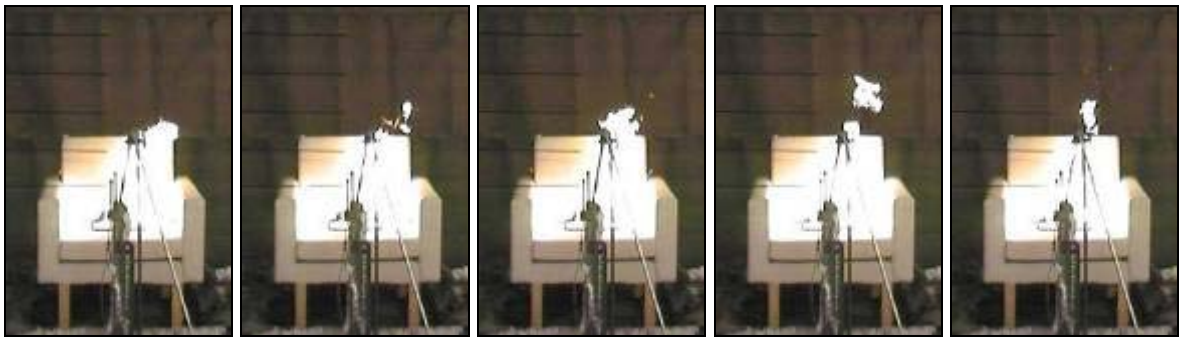

Figure 3-6 – Series of 'Chair 16' Images before Image Manipulation

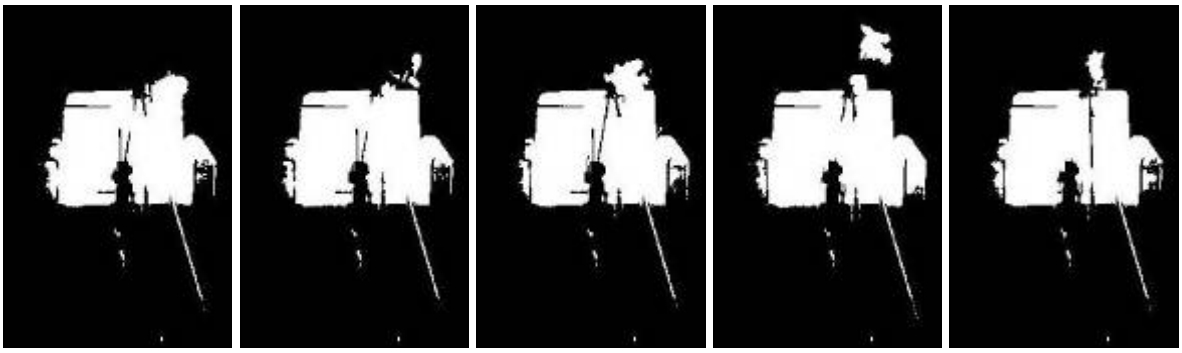

Figure 3-7 – Series of 'Chair 16' Images after Image Manipulation (from Figure 3-6)

Figure 3-8– Average of Five Images (from Figure 3-7)

Averaging 150 images results in an image containing the locations and probabilities of the flame existing in certain areas of the frame over 6 seconds. 6 seconds was chosen because Mason showed that it takes this long for the image to give "a true picture of flame probability", while much longer than this results in decreasing probabilities throughout the image, due to the shifting nature of the flame. Averaging 150 frames results in an image such as Figure 3-9:

Figure 3-9 – Typical Resulting Image from Averaging 150 Frames (6 seconds) of Video Footage

3.3 Flame Reconstruction

There are two possibilities for reconstructing flame images into 3 dimensional representations: locating flame position or extracting flame intensity information. Mason gave the reasons why accurate flame intensity data is unattainable with a standard video camera because of the way incoming light is turned into a digital reading. His reasoning is summarised below.

As mentioned earlier, a transfer function relates the amount of light entering each well to the resulting pixel intensity. This transfer function is generally non-linear, and even though some video cameras allow the so-called gamma correction to be turned off it is usually fixed by the manufacturer and not specified. Accurate flame intensity measurements are therefore difficult to obtain, which is the reason flame location (determined using the thresholding techniques described above), and not intensity, was studied in his report and is here as well.

3.4 Minima Reconstruction Technique (MRT)

The camera position and two reference points in each image (P_1 and P_2) must be given in relative real world coordinates. The coordinates of the screen reference points can be located by a computer. An example of the data required for two orthogonal videos is given below. Only part of each image is shown to magnify the areas of interest. Note that in screen coordinates, the y-direction is positive downwards and the x-direction is positive to the right. The z-direction in screen coordinates is positive moving away from the user, but obviously only one plane can be shown. An example of the reference points chosen for two videos of a furniture fire is shown as Figure 3-10 below. Table 3-1 contains the screen and real world coordinates of the reference points as well as the real world position of the camera.

Note that each image is considered independently, and for the purposes of creating a computer program, each image must be associated with a distinct P_1 and P_2, as well as a unique camera position. As is shown in Figure 3-10, it is often convenient to locate the same physical point in two separate images (for instance, the corner of a seat cushion). It is also quite valid to call this point P_1 for one image and P_2 in another for ease of inputting into a computer programme.

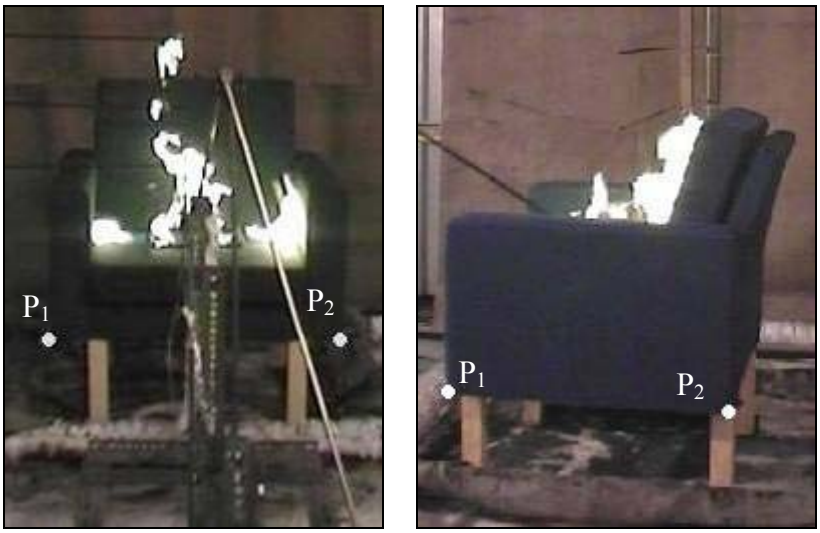

(a) **(b)**

Figure 3-10 – (a) Front View (b) Side View of 'Chair 15'. White Circles are Reference Points.

Table 3-1 – Reference Points for 'Chair 15' and 'Chair 16' Videos in (x, y, z) format. x is positive towards the front camera, y is positive towards the ceiling and z is positive towards the side camera

Reference Points	**'Chair 15' Front (mm)**	**'Chair 15' Side (mm)**	**'Chair 16' Front (mm)**	**'Chair 16' Side (mm)**
$P_{1, screen}$	(226, 558, 0)	(156,606,0)	(224,593,0)	(169,606,0)
$P_{2, screen}$	(369, 586, 0)	(349,621,0)	(375,593,0)	(365,619,0)
$P_{1, world}$	(-375,250,-300)	(375,250,-300)	(-375,250,-300)	(375,250,-300)
$P_{2, world}$	(375,250,-300)	(375,250,300)	(375,250,-300)	(375,250,300)
Camera	(0,1405,4470)	(2880,1080,0)	(0,1405,4470)	(2880,1080,0)

The manipulated image is then projected through a point cloud. A 3-dimensional point cloud is established above the region of interest (i.e. the region above and including the burning item). The points in the cloud can be spaced at regular or irregular intervals. For our purposes we have assumed a regular grid, however to gain greater accuracy for flame height calculations at a relatively low point cloud density, an irregular (random) grid would have been more appropriate to allow greater resolution of the flame tip. Using an irregular grid, the resolution of flame height is limited to the density of the point cloud, rather than the discrete grid step size. A regular grid size is the quickest method of calculating the volume of the 3

dimensional representation as the number of points in the final point cloud can be multiplied by the volume of individual cells in the point cloud. With an irregular grid, calculating the average distance between points would be the only method of determining the flame volume.

Each pixel in the final image has a greyscale value that relates that position to the probability of the flame existing at that location. This probability is projected through the point cloud from one direction, and the point cloud retains the values of the projected pixels. The second image is projected from another direction, depending on the coordinates of the reference points and the second camera. This time the point cloud retains the lower probability of the first or second image. Points having 'zero' probability are discarded. A surface function was fitted at this point in Mason's work, enabling the radiative heat flux away from the flame surface at a certain probability to be calculated. For reasons explained later this was not done for this research.

The point cloud is analysed to determine its volume and height for this thesis. Since we have stated that the distance between points in each direction in the cloud will be constant, we can determine the volume described by each point. The total volume is then the number of volume elements multiplied by the single point volume.

$$V_{\text{single point}} = \frac{(X_{\max} - X_{\min})}{N_x} * \frac{(Y_{\max} - Y_{\min})}{N_y} * \frac{(Z_{\max} - Z_{\min})}{N_z} \tag{12}$$

The number of points in each direction, N_x, N_y and N_z do not have to be equal. In fact, when locating the flame tip it is a good idea to increase the number of points in the y-direction to increase precision.

3.4.1 Grid Size

As with many analytical techniques, increasing the accuracy of the method also increases the computation time required. Performing the techniques described here on a single fire with a reasonable degree of accuracy could require a computer with a 500 MHz processor to run for up to 5 days. The long time taken to run the MRT program for a single video with a reasonable amount of accuracy was the reason more video footage was not analysed. More footage of furniture fires is available could be easily analysed by a faster computer for a future project. The time required in order to run the entire MRT program (including operator input time and converting the video footage into useable greyscale images) was

approximately 5-7 days. The process of running the programs created is described in detail in Appendix B.

Increasing the number of points in each direction (x, y, z) greatly increases computational time. For instance, changing the number of points in the grid from (10, 10, 10) to (20, 20, 20) increased the time taken to analyse one frame of a video from 46 to 240 seconds. Since there are 7500 frames in a 5 minute video, this represents a large increase in computation time.

Mason described a procedure for using a Butterworth Low-Pass Filter to determine whether the point cloud is dense enough to avoid aliasing, which "occurs when a reconstruction produces from a sample does not accurately represent the underlying information". He found that a sampling rate of every 5 pixels was sufficient to prevent aliasing.

Our point cloud was established in the grid:

$(X_{min}, X_{max}) = (-0.375, 0.375)$

$(Y_{min}, Y_{max}) = (0, 2.20)$

$(Z_{min}, Z_{max}) = (-0.30, 0.30)$

When the flame height was being determined, to increase the resolution nearer the flame tip, the y-direction was established with the limits:

$(Y_{min}, Y_{max}) = (0.50, 2.20)$

Since the smallest flame height determined was 0.55 m, this minimum flame height was sufficient to capture all the flame heights. If the smallest flame height was 0.50 m, re-evaluation of this lower limit would be necessary.

The x and y-components of this grid correspond to approximately 180 x 300 pixels.

The number of points in each direction was: $(N_x, N_y, N_z) = (12, 17, 12)$ for the flame height and flame pulsation frequency grids and (20, 20, 20) for the flame volume grids. For the flame height and pulsation frequency grids, there are more points in the y (vertical) direction to gain a better resolution of the flame tip. Therefore, the minimum point cloud density was 300/17 = 18 pixels. This indicates that the sampling frequency used in this thesis was too low. Increasing the point cloud density to 60 sample points over these 300 pixels would

increase the processing time from 5 – 7 days to 2 – 3 weeks on a similar computer. For practicality, examining only a section of the video would be necessary in this case.

3.4.2 Transformation from Screen to World Coordinates

To enable a 3-dimensional representation to be created, reference points must first be located in each image. However, since each video file is assumed to be stationary, this means that the reference points are only located once for each video. The real world location of two points in an image as well as the real world location of the camera lens viewing each image allows the computer to create a scaling matrix to translate a pixel location from screen coordinates into a real-world position.

A transformation matrix, $M_{combined}$, describes the conversion between 3-dimensional world coordinates and 2-dimensional image coordinates. The transformation is made up of three components – scaling, translating and rotating. Mason describes the derivation of these matrices and comes up with the following equations. VRP stands for the View Reference Point, which is taken to be the centre of the image as specified in world coordinates. The vector **n** is the vector from the camera to the VRP and defines the orientation of the image (viewing plane). **v** is the viewing plane's up vector, and the vector **u** is the cross product of **n** and **v**. The orthogonal vectors **u**, **v** and **n** define the axes of the viewing coordinate system.

$$\text{Rotation: } R = \begin{bmatrix} u_x & u_z & u_z & 0 \\ v_x & v_y & v_z & 0 \\ n_x & n_y & n_z & 0 \\ 0 & 0 & 0 & 1 \end{bmatrix} \tag{13}$$

$$\text{Translation: } T = \begin{bmatrix} 1 & 0 & 0 & -VRP_x \\ 0 & 1 & 0 & -VRP_y \\ 0 & 0 & 1 & -VRP_z \\ 0 & 0 & 0 & 1 \end{bmatrix} \tag{14}$$

$$\text{Scaling: } M_{scale} = \begin{bmatrix} 1 & 0 & 0 & 0 \\ 0 & 1 & 0 & 0 \\ 0 & 0 & 1 & 0 \\ 0 & 0 & 1/z_{cv} & 1 \end{bmatrix} \tag{15}$$

Combined Transformation: $M_{combined} = M_{scale} RT$ (16)

The unknowns in the above equations are:

VRP, the View Reference Point (the origin of the viewing plane)

n, the vector from the camera to the **VRP**

v, the viewing planes 'up' vector

u, which equals **n** x **v**

Mason describes a 5-step approach to finding the unknowns in order to make the transformation from viewing to world coordinates.

1. Locate the camera C_v in viewing coordinates
2. Find P'_{1w} and P'_{2w} in world coordinates
3. Find **VRP** in world coordinates
4. Find the up vector, **v**
5. Assemble the matrices and multiply them to get the transformation

Mason describes in detail how to determine these unknowns. This will not be repeated here.

Therefore, from knowing the position of two artefacts in the screen (such as the top of a chair arm), the location of all points in the image can be given approximate real world coordinates.

Each point in the cloud is initially assigned a probability of 100%. One at a time, the averaged images from the two orthogonal camera views are passed through the point cloud. Two images are transformed to show the shape of the resulting 3-dimensional point cloud. Figure 3-11 is an indication of the resulting shape from projecting one equilateral triangle from the front view and two isosceles triangles from the side. Note that probabilities are not included in this diagram.

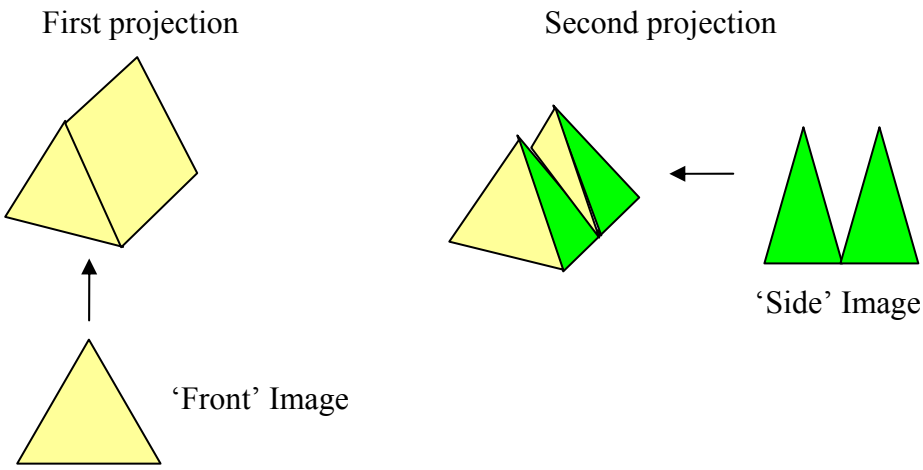

Figure 3-11 –Resulting shape of a 3-dimensional point cloud after projecting two orthogonal images

If the value of the pixel in the averaged image is less than the point cloud value it is projected through, the lower value is retained at that point in the point cloud. If the value projected is 0 (no flame at this point) the point is discarded to reduce computer memory requirements. This means parts of the point cloud are discarded due to there being no flame in part of the image being projected. Once the first image has been projected, the second follows, again replacing any point in the point cloud with a lower projected value. This will result in a point cloud such as Figure 3-12 which has been output into a VRML file along with the VRML code required to create a 'chair'. VRML stands for Virtual Reality Mark-up Language, which can be written using a text editor to describe 3-dimensional objects and worlds by defining a series of points and the way each point connects to others in the object. Colour and lighting effects can also be added. A freely downloadable web browser add-on such as 'Cortona' or 'Cosmo Player' [9] can be installed to enable Microsoft Internet Explorer or Netscape Navigator to view and explore the VRML world. One can see the discrete levels of flame heights because of the regular grid spacing.

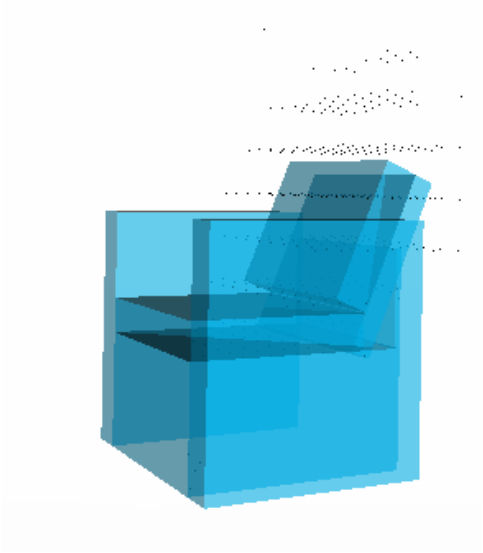

Figure 3-12 – VRML representation of point cloud and 'chair'. The chair is included only to give a sense of scale and location.

At this stage in Mason's work, a radial basis function was fitted to the point cloud. This had the following benefits:

- The radial basis function allows fitting of a surface to the outer points in the cloud with certain probabilities, enabling a series of volume shells to be defined from between 0% and 100% probability (i.e. the shell contains all points with a probability higher than 0% or 100%, respectively)

- Calculating the area and orientation of each surface of the radial basis function allows radiation shape factors to be calculated. With an estimate for the flame temperature, a shell of constant heat flux could be constructed to determine, for example, whether a nearby object would be subject to sufficient heat flux to ignite.

- The radial basis function allows areas which are obscured by other objects such as measurement instruments and chair arms to be filled in. These objects result in a null value being projected through the point cloud, even though the flame may be at its most intense on the other side of the object and recorded by another camera. Using a surface interpolation tool such as the radial basis function fits a surface over the 'missing' data which is similar to that expected if the object did not obscure one camera's view.

- The radial basis function provided a visual result – VRML output similar to that in Figure 3-13 displaying the flame 'surface' can be created using the commercially available radial basis function software 'FastRBF Toolbox'.

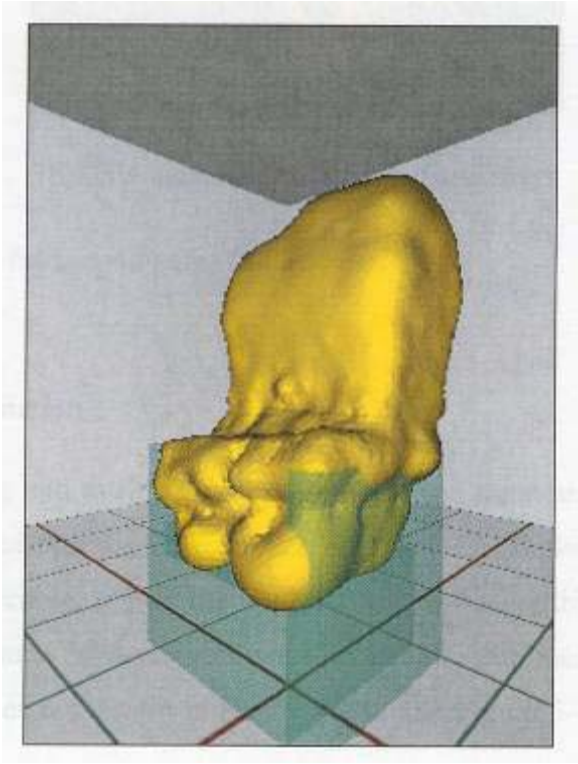

Figure 3-13 – VRML output including radial basis function surface. Picture taken from Mason, 2003.

For our purposes, we are attempting to provide a readily available set of analysis tools without the need for buying additional software packages. Radial basis function software such as the FastRBF Toolbox costs several thousand NZ$ so is not used in this analysis. We are, however left with the problem of defining flame volumes and presenting visual data without the use of the radial basis function. Objects such as a chair arm obscuring one camera's view of the flame will result in a complete volume slice being taken out of the image, which may have little effect on the flame height calculation, but will likely influence the volume calculation greatly.

There is no simple, automated way of reducing this effect without the use of the radial basis function or similar tool. One suggestion this author has is to create a software tool which allows the user to 'block out' a section of a thresholded image (eg masking a section of the image, say the arm of a chair with a white rectangle), with that section being added to all the other images. This will likely lead to an overestimation of the flame volume, especially in earlier or later stages of a furniture fire when the flame will not be as intense on the other side

of this object, but this will probably lead to a safer design tool than the current underestimation in flame volume, as this will lead us inexorably to a higher flame volume to heat release rate value.

3.4.3 Sampling Frequency

For their work involving measurement of flame height, Simard et al. (1989) indicate that while a sample interval of 1 second may be adequate for determining mean and standard deviation flame heights, a sample interval of 0.05 seconds is "probably needed to accurately measure maximum flame height, [and] pulsation rate…" As we are attempting to investigate these two effects using readily available video equipment which is capable of recording 25 frames per second, we are just able to meet this criterion for sufficient measurement accuracy. Therefore, when determining mean flame heights in this thesis, moving averages involving one second of data will be used. Individual frames taken every 0.04 seconds will be required for determining accurate flame tip locations.

For analysis of the flame height results it will be assumed that the mean flame height comprises a 25 point moving average of the determined flame heights. This corresponds to 1 second of video footage and is approximately the maximum time period given by Simard for gaining mean flame heights.

For the work involving determining flame volume, there is difficulty in exactly synchronising two orthogonal views of a fire. This may lead to an underestimation of the flame volume. To avoid this, a 6-second 'average' of the video footage is taken. This time period was proposed by Mason and allows flame pulsation and leaning due to air currents to average out, while not allowing the size of the fire to change markedly.

Chapter 4

Flame Height

4.1 Calculating Flame Height from Video Footage

Two alternative methods for determining flame height from video footage are proposed:

- Perform the MRT on single frames of video footage from multiple angles. It is quite likely, however, that the two videos of the fire will not be perfectly synchronised since the two video cameras were set to record independently. This means that it is difficult to tell exactly which frame from each camera should be used, which will almost certainly lead to an underestimation of the flame height due to the way the minima reduction technique favours pixels with a 0-value (i.e. black) over all others.

- Perform the MRT on single frames of video footage from a single angle; that is, fool the software into thinking it is analysing two orthogonal views of the fire by changing the x and z-components of the camera position. Incorrect calibration and synchronisation errors should be minimised.

The point cloud resulting from running the minima reduction technique algorithm on individual frames of the fire is analysed to locate the top plane containing at least 6 points to remove the possibility that a very small part of the flame or reflective surface is located. This plane is taken to be the height of the flame for that individual frame. This height is relative to the origin in the coordinates fed to the MRT computer program and may need to be adjusted to give the true height above the burning surface. For instance, at the start of a furniture fire experiment, the base of the flame is at the height of the seat cushion. During the experiment, molten foam pools below the chair and after approximately 3-4 minutes the chair is almost totally consumed by fire, with the base of the flame being quite clearly on the ground below the chair. Between these two extremes, it is more difficult to accurately locate the base of the flame. More discussion on this problem is given in Section 4.6 below.

If the point cloud was not regular, another method would need to be chosen to determine the flame tip location, as the top points in the point cloud would no longer be in the same plane.

It would be slightly simpler to determine the height of a flame from one image without projecting the image using the minima reduction technique, however this may result in any reflective surfaces being misinterpreted as the height of the flame by a computer program.

4.2 Furniture Fires

Several items of upholstered furniture were burnt in the furniture calorimeter as part of Hill's (2003) research. The sample is ignited at the start of the experiment and the ignition source, a LPG ring burner with a constant heat output of 30 kW is removed after 2 minutes. Therefore, after the initial ignition period, the only radiation incident onto the sample is from the flame itself. As the name suggests, the furniture calorimeter is most often used for gaining the burning properties of large items, such as upholstered furniture, wooden pallets, and items as large as automobiles.

Two video cameras were used during the experiments. The flame height of one furniture fire is examined in detail in this section. For completeness footage of another furniture fire is analysed, however it is stressed that much more footage exists to be analysed. The large amount of time taken to process each video is the reason more footage was not analysed. The reconstruction technique was used on individual frames of the videos to gain flame height information every 0.04 seconds. This was done several different ways as described above. The chair dimensions and characteristics can be found in Appendix A.

4.3 800mm Pool Fire

A series of pool fires with diameters from 0.1 to 0.8 m were videoed. The video of the largest of these was deemed suitable for analysis using the techniques described here. The other videos contained too much reflection from surfaces behind the flame. The height of the intermittent and continuous flame regions was estimated using McCaffrey's criteria based on an estimated heat release rate. Since only a single video was taken the fire is assumed to be axisymmetric and the same video is projected from two orthogonal 'directions' to give the 3-dimensional representation.

4.4 Furniture Fire Flame Height Results

Figures 4-1 to 4-3 show the flame height over approximately 5 minutes of burning for the experiment labelled 'Chair 16' conducted by Hill at the University of Canterbury in 2003 .

Graphs of the flame height vs time as calculated using the two methods above follow. The heat release rate is plotted alongside to give an idea of the size of the fire.

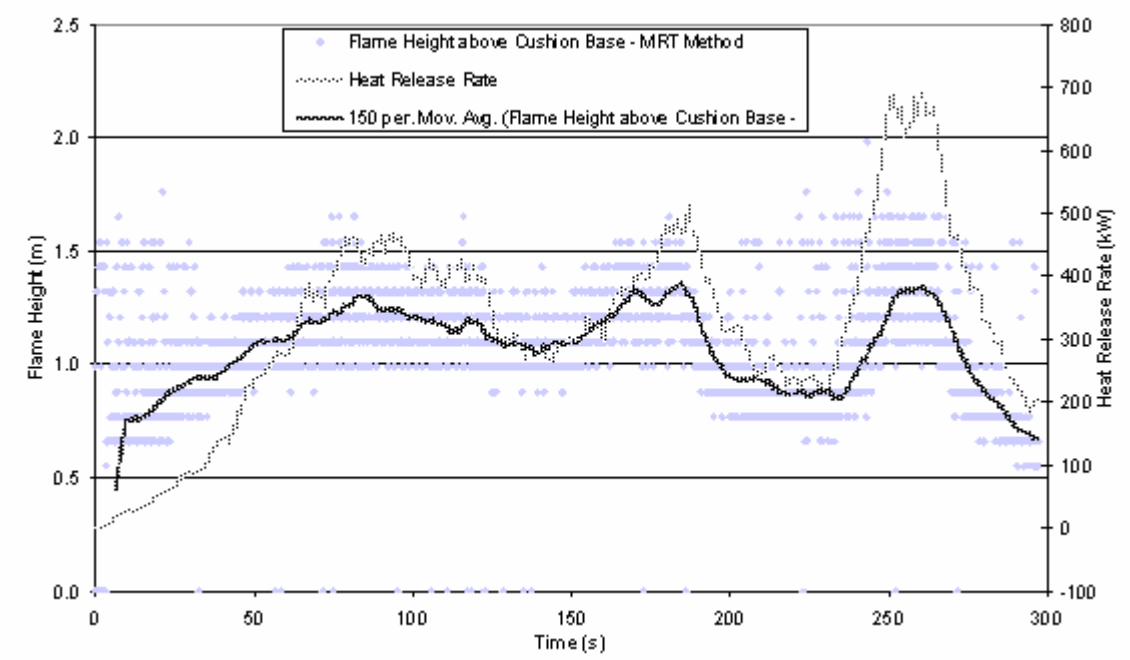

Figure 4-1 – Flame height vs time for 'Chair 16' – front view of fire projected from both sides

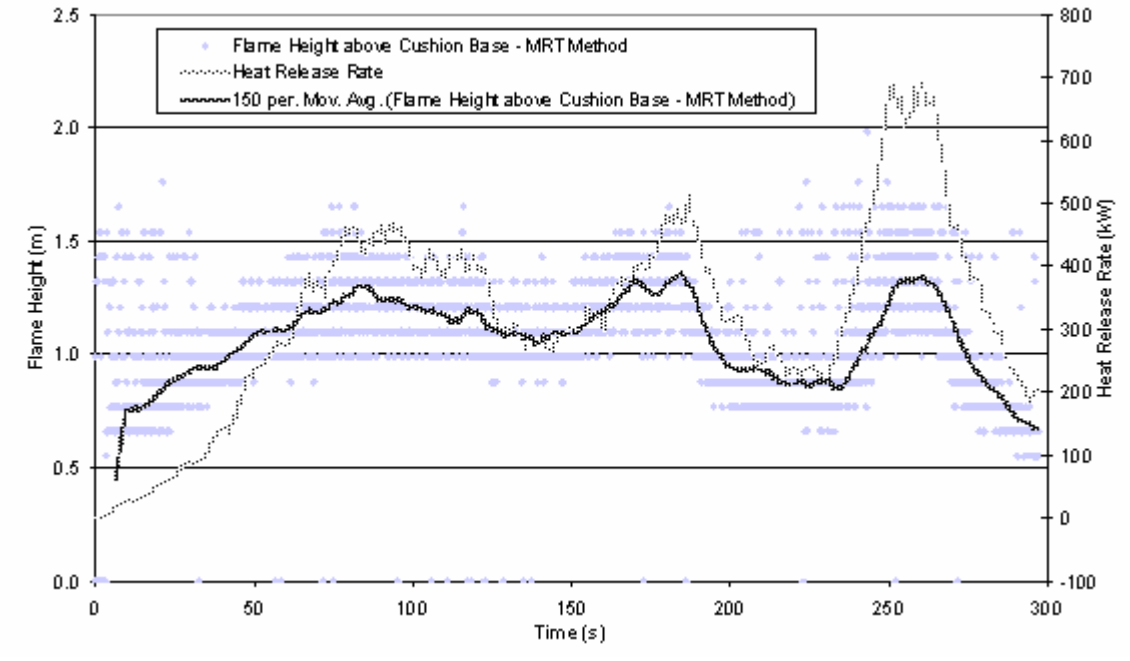

Figure 4-2 – Flame height vs time for 'Chair 16' – side view of fire projected from both sides

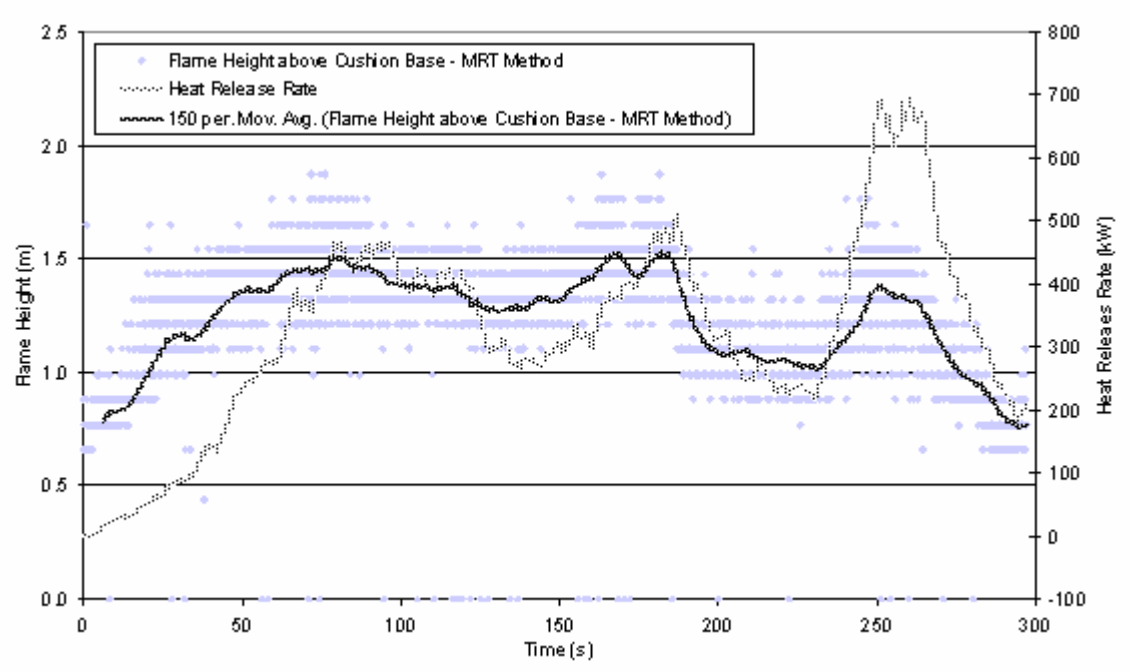

Figure 4-3 – Flame height vs time for 'Chair 16' – front and side views of fire projected

The video taken from the front of the experiment 'Chair 15' was projected in the same way. The results are shown in Figure 4-4. As mentioned earlier, this chair was not examined in as much detail as the 'Chair 16' videos due to time considerations. Again, the heat release rate as determined from furniture calorimeter measurements is plotted alongside the flame height data.

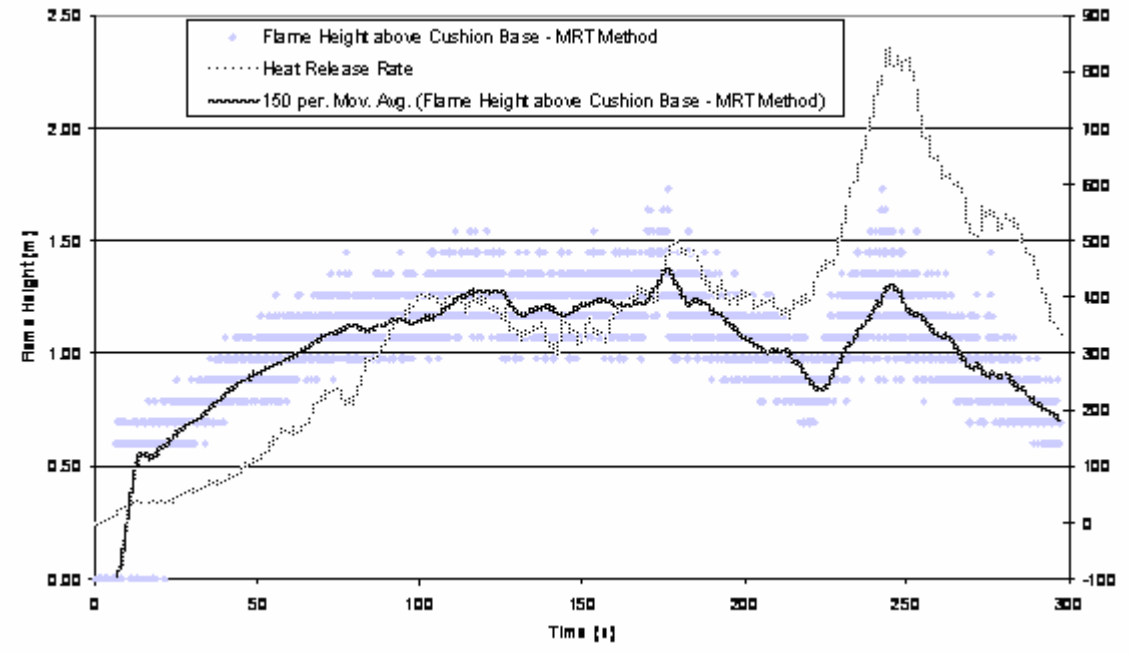

Figure 4-4 – Flame height vs time for 'Chair 15' – front and side views of fire projected

4.4.1 Mean Flame Height Comparison

Equation (4) is used to estimate the mean flame height for the experiment 'Chair 16' using the experimental heat release rate and an estimated base diameter of 0.8 m, which is approximately the largest dimension of the base of the seat. An average value was chosen as the flame diameter was not determined as part of the analysis. Figure 4-5 compares this to the 150 point moving average obtained from projecting the front and side views of the fire using the minima reduction technique.

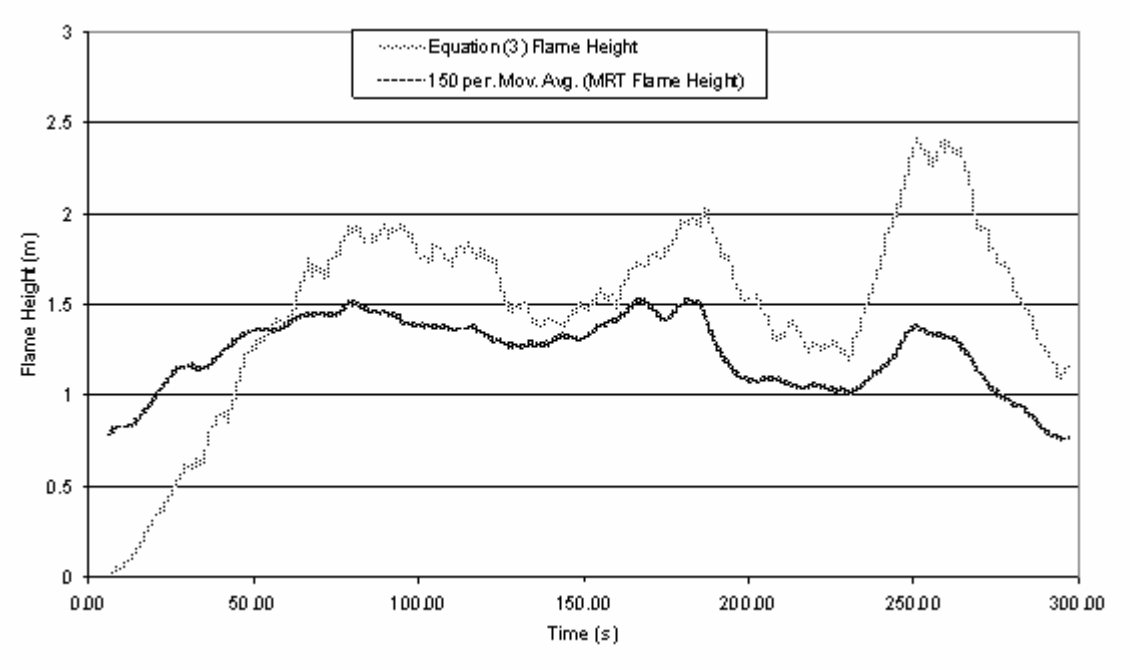

Figure 4-5–Comparison between 'Chair 16' 150 point moving average for flame height from MRT and average flame height estimated using Equation (4) from experimental heat release rate data and using D = 0.8 m.

4.5 0.8 m Poolfire Results

Figure 4-6 shows the result of using the MRT to determine flame heights for a 0.8 m diameter methanol poolfire. Two seconds of results are shown in more detail in Figure 4-7.

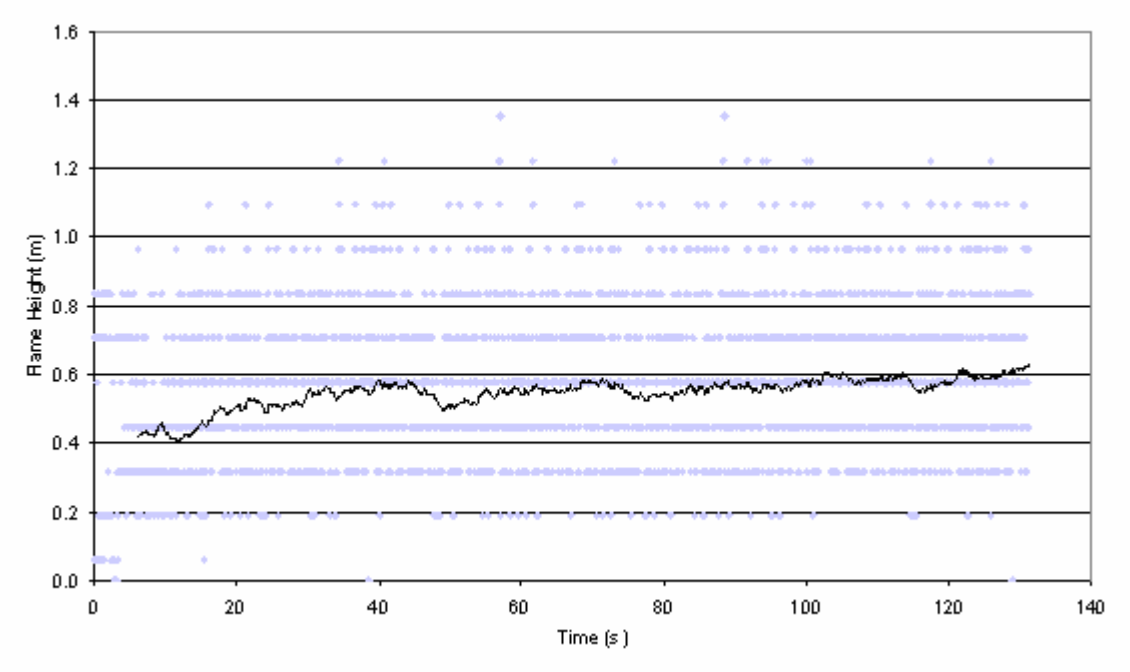

Figure 4-6 – 0.8 m Diameter Poolfire Flame Height

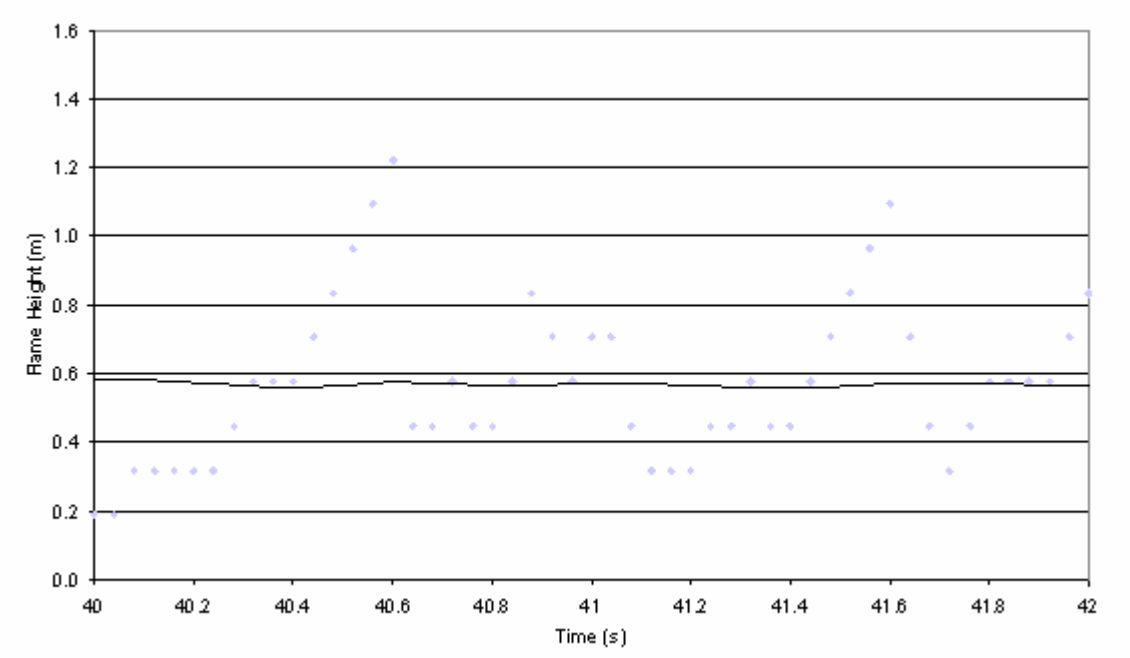

Figure 4-7 – 0.8 m Diameter Poolfire Flame Height – Detail Shown From 40 to 42 Seconds

Excel was used to determine the flame height maxima and minima over 25 frame intervals (1 second). Figure 4-8 shows the results of this plotted against McCaffrey's estimated intermittent and continuous plume heights

The heat release rate for this 800mm diameter pool fire can be estimated using Equation (17):

$$\dot{Q} = A_f \dot{m}'' \chi \Delta H_c \tag{17}$$

Here A_f is the area of the fire ($=\pi/4*(0.8)^2 = 0.50$ m^2), $\dot{m}''$ is the free burn mass loss rate (kg m^{-2} s^{-1}), χ is the combustion efficiency (estimated to be 1 as methanol is clean burning) and ΔH_c is the heat of combustion for methanol, 20.0 MJ kg^{-1} (Karlsson and Quintiere, 2000.)

For non-alcochol pool fires, the free burn mass loss rate is estimated by Equation (18) which considers the diameter and the asymptotic diameter mass loss rate, $\dot{m}''_\infty$, which has been found to be 0.017 kg m^{-2} s^{-1} for methanol (also from Karlsson and Quintiere, 2000.)

$$\dot{m}'' = \dot{m}''_\infty \left(1 - \exp\left(-k\beta D\right)\right) \tag{18}$$

For alcohol-fires such as methanol or ethanol, the free burn mass loss rate is estimated based on the diameter as follows:

Diameter, D (m)	Free burn mass loss rate $\dot{m}''$ (kgs^{-1})
< 0.6	0.015
0.6 < D < 3.0	0.022
3.0 < D	0.029

$\dot{m}''$ is therefore estimated to be 0.022 kg m^{-2} s^{-1} and $\dot{Q}$ is therefore calculated to be 220 kW.

The heights of the continuous and intermittent regions of the flame were estimated as 1.73 m and 0.69 m, respectively using McCaffrey's criteria and using the 220 kW estimate of the heat release rate. The 'intermittent' and 'continuous' flame heights were determined to be the maximum or minimum determined flame height over a period of 25 frames (1 second of video footage).

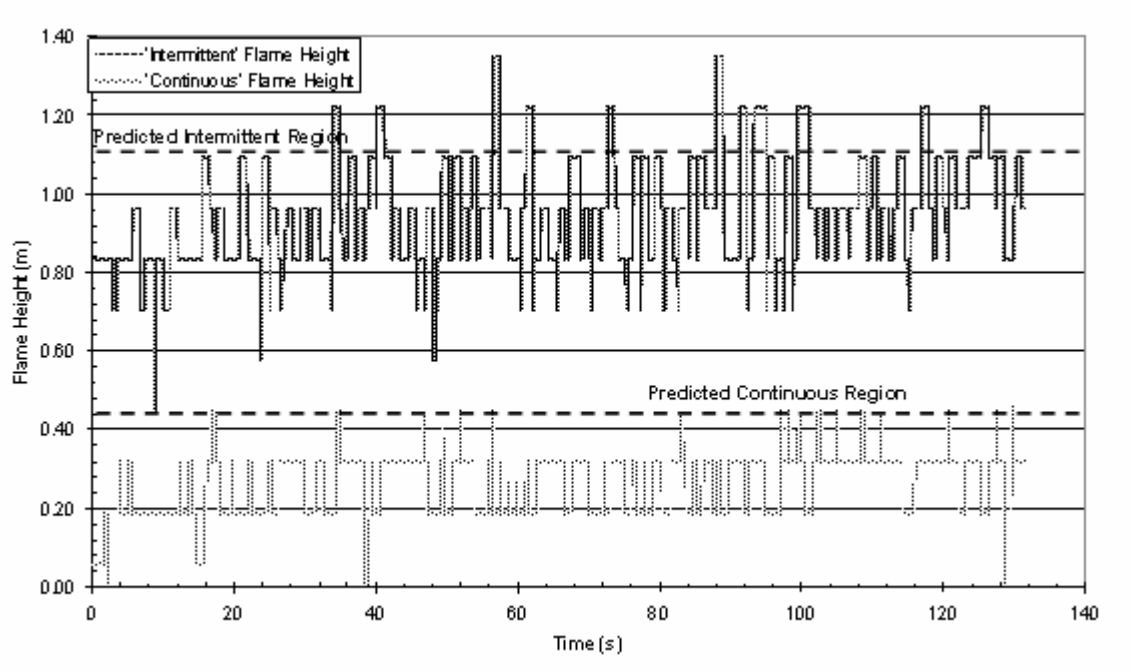

Figure 4-8 – Predicted and MRT-determined height of continuous and intermittent flame regions for a 0.8 m diameter methanol poolfire

4.6 Discussion of Furniture Fire Flame Height Results

Unfortunately, this author was not present when the furniture fire experiments were performed and distance measurements were not taken during the experiment. Therefore, the relative position of the camera lens to the reference points in each frame was only estimated for use in the above analysis. The position of the screen reference points was determined using knowledge of the dimensions of the chairs (see Appendix A) and known positions of items from other video footage. This could be lead to flame heights being underestimated by the techniques presented here.

From Figure 4-5, the mean flame height estimated from Equation (4) is generally greater than the 150 point moving average. This may indicate that the MRT method has difficulty locating the tip of the flame. As with most of the results here the general trend of the graph is the same in both cases with major peaks forming at around the same time which is an encouraging result. Fine-tuning of the inputs into the MRT program, such as the correct threshold level and colour plane to extract from the video images may be necessary.

The flame heights determined from projecting the front view from both directions led to the generally lowest average flame heights. A possible reason for this is that the tip of the flame

from the front view may have been narrow, but was wider from the side. Since the flame height was defined as the top plane in the point cloud containing at least 6 points, this would lead to a projection of the front view creating a very narrow tip which is not identified by the program.

The changing position of the base of the flame was not investigated. It was decided it would be too difficult to write a program that could accurately locate the base of the flame for a furniture fire especially as the foam melts and drips below the base of the seat, forming a pool fire and a second peak in the heat release rate. Figure 4-9 is a good indication of this – in one image, there are small pockets of flame beginning to form below the seat of the chair and the side of the chair arm has just caught fire. In the next image, the dripping foam has formed a pool fire at the base of the seat – clearly the position of the base of the flame. It is difficult for a human to decide what constitutes the base of the flame given three choices – the base of the seat, the bottom of the chair arm, or the ground where the pool fire is beginning to form; it is much more difficult to design a computer program to do this.

For this thesis, the base of the flame was taken to be the top of the seat cushion on the chair throughout the analysis, rather than requiring a user to input the location of the base of the flame in every frame. An alternate method would be to give the base of the flame as either the seat cushion or the base of the chair depending on whether the first or second peak in heat release rate had been reached. With a furniture fire, there are often two peaks in heat release rate. During the second peak, the flame formed by melted foam dripping to form a pool seems to consume the entire chair. At this point, the base of the flame could be considered to be at the base of the chair. This argument presents a strong case for determining the flame height from all available views of the fire to avoid missing information such as the burning side of the chair.

Again, since the methods developed in this thesis are supposed to be flexible enough to be used in the field where there is neither time nor sufficient facilities to measure the heat release rate (and the fire would probably not comprise only of a piece of furniture), other means will be necessary to locate the base of the flame for each case examined.

Figure 4-9 – Two Front Views of 'Chair 15' Showing the Varying Degrees to which the Flame Base may be Located at Positions other than the Top of the Seat Cushion.

4.6.1 Random Checking of Flame Height Results

To ensure accuracy of the MRT method, a randomly generated sample of 10 frames was taken from the front view of 'Chair 16'. The flame height is estimated by eye using the constant spacing between thermocouples to the left of the flame as a guide to the flame height. The flame heights are compared to the flame heights measured using the MRT method as shown below in Figure 4-10.

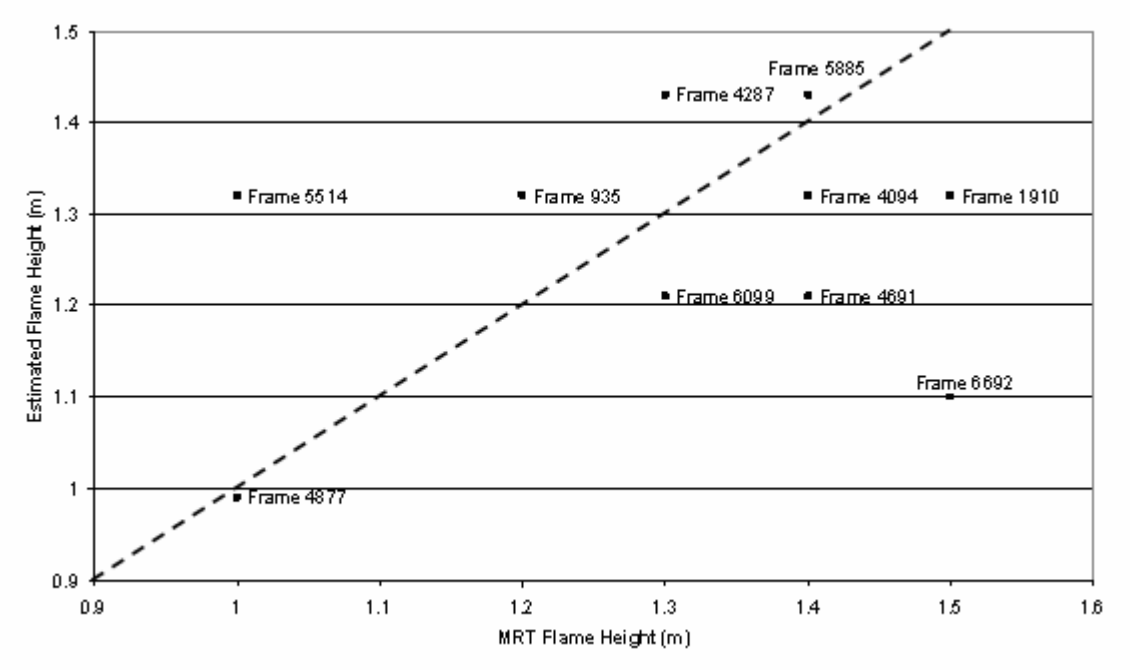

Figure 4-10 – Discrepancies between MRT-Determined and Estimated Flame Height for a Random Sample of 10 Video Frames.

Obviously there is some disagreement between the results, however it is difficult to estimate the flame height accurately by eye (the estimated height is based on the assumption that there is 0.2 m between each of the thermocouple probes visible in each frame), and using a regular grid in the minima reduction technique leads to discrete flame heights (in this case the minimum flame height resolution is ±0.11 m.) All but two of the estimated results above lie within 2 discrete flame height levels (i.e. within 0.22 m) of the MRT results. Frame 6692 had the greatest discrepancy of all those tested. This frame is shown below and shows the difficulty faced in estimating the flame height by any method – it is difficult to determine where the flame tip lies, as there is a disconnected piece of flame that does not have the same intensity as the rest of the flame so will likely be missed by the image processing technique. Changing, for instance, the lower threshold value input from 140 to 180, say, would alter the final flame height determined (See Figures 4-11 and 4-12.) The flame tip in Figure 4-12 (b) is slightly narrower and therefore more likely to be missed by the MRT, especially with a coarse grid size, leading to a lower flame height.

Figure 4-11 – Frame 6692 from 'Chair 16' experiment showing difficulty in determining position of flame tip.

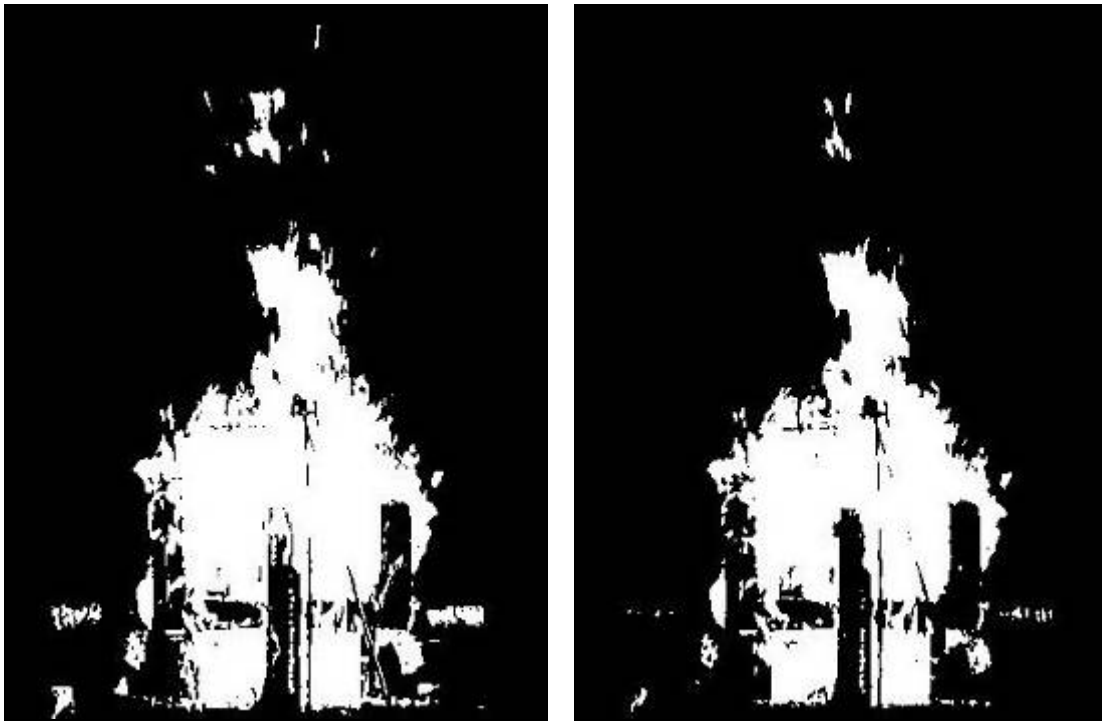

(a) **(b)**

Figure 4-12 – Thresholded value of Frame 6692 from 'Chair 16' experiment after extracting 'Luminance' colour plane. Lower Threshold Values: (a) = 140; (b) = 180.

4.7 Discussion of 0.8 m Poolfire Flame Height Results

Both the predicted intermittent and continuous regions were consistently higher than that measured by the MRT method. This is a strong indication that the method was unable to detect the height of the flame with any accuracy, however it is possible that the user over-compensated for the reflective background in the video images by setting a high threshold value when extracting the binary images from the greyscale images for this particular fire. This is another reason why it is advantageous to film the fire from more than one direction, as the minima reduction technique would discard the reflected surface if it did not appear from both directions.

Chapter 5

Flame Pulsation Frequency

5.1 Background Information

Flame pulsation frequency is investigated herein using the same techniques developed for determining flame height, whereby the position of the "flame tip" in individual video frames is located. In the previous chapter this information provided a means of determining the height of the so-called "continuous" and "intermittent" regions of an uncontrolled buoyant flame. As the flame flickers, the region between the upper and lower bounds of the flame tip would fit the description of the intermittent region of the flame, using the terminology of McCaffrey (1995) for a buoyant axisymmetric fire plume. McCaffrey divided this type of flame into continuous, intermittent and buoyant plume regions (See Figure 5-1.)

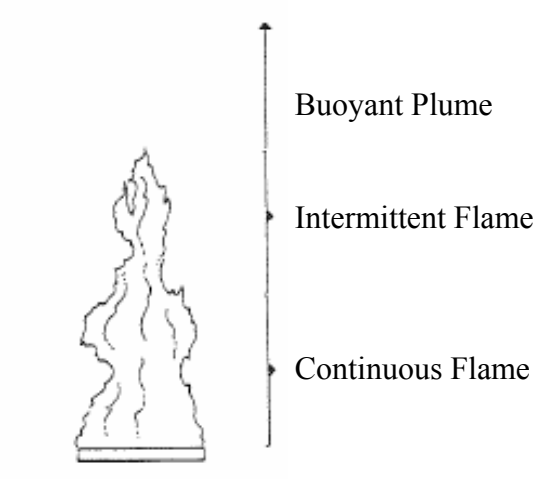

Figure 5-1 – McCaffrey's definitions of Continuous, Intermittent and Plume regions of an Buoyant Axisymmetric Fire Plume. Image taken from Karlsson and Quintiere (2000).

Below the minimum height of the flame tip is the continuous region and above the maximum is the plume region. The area between the maximum and minimum flame tip positions is then the intermittent region. The flame size changes markedly during the furniture fire experiments from that just involving the burner at the start of the experiment to that involving the entire chair from the ground up. It is again proposed here that the minimum flame height over a period of 1 second would be the location of the top of the continuous region and the maximum of these flame heights would be the bottom of the intermittent region for determining the flame pulsation frequency. This period again relates to the one second

maximum sampling period given by Simard et al. and should allow the flame sufficient time to flicker between its maximum and minimum height while there is a relatively constant flame diameter – in other words, the maxima and minima should be unaffected by the changing size of the fire. Other time periods for the average have been investigated here, as the period of flame flicker is likely to be on the order of 1 second, and the technique may miss the true pulsation frequency if the average flame height is changing with the same time period.

The techniques developed here will be used to examine the pulsation frequency and compare the results to the correlation given by Cox and Malalasekera (Equation 8).

As stated earlier flame pulsation frequency has widely been reported as being from 0.4 to 10 Hz for typical fires (with results for pool fires and furniture fires in this range) while candles have pulsation frequency of approximately 10-11 Hz (Cox, 1995).

5.2 Minima Reduction Technique for Flame Pulsation Frequency

Using the flame height results for the furniture fire 'Chair 15' and 'Chair 16' from Chapter 3, the pulsation frequency for these fires is calculated. Again only single frames of the video footage are used in the MRT technique instead of the 6 seconds worth of footage (150 frames) used by Mason for his research and for the volume calculations we perform later. Again the flame height results were calculated by using the minima reduction technique on video footage shot from both sides, or by using the same footage and projecting it from two directions for 'Chair 16'. The pulsation frequency for 'Chair 15' is only determined from video footage from one direction (from the front).

5.3 Determining Flame Pulsation Frequency

Two methods were trialled to find the flame pulsation frequency. One such method involved Fourier transforms of the flame height result time series. It was thought that by performing a Fast Fourier Transform (FFT) on the furniture fire flame height results the period of oscillation could be extracted. However since the flame position is such a dynamic turbulent feature, the FFT was unable to resolve the pulsation frequency, returning a range of possible pulsation frequencies with similar magnitudes that indicated the period of each pulsation could lie between 0 seconds and the length of all the data given. The result of performing a Fast Fourier Transform on the 'Chair 16' results is shown below.

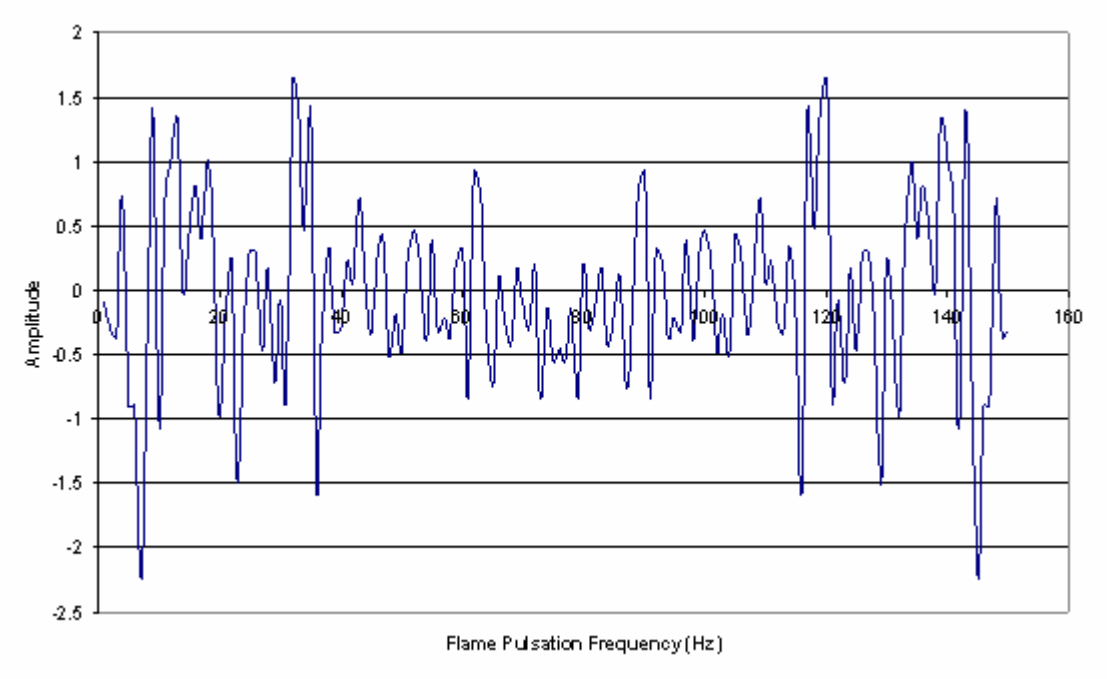

Figure 5-2 – Results of Performing a Fast Fourier Transform on Flame Height Results to Determine Flame Pulsation Frequency

Microsoft Excel was used to determine the flame pulsation frequency for the furniture and pool fires. The technique used was as follows:

- Calculate a 25-point moving average of the flame height. Since the camera takes 25 frames-per-second, this corresponds to 1 second of data. It was thought that, over 1 second, the average flame height would not change significantly due to the changing fire size.

- For each individual frame, determine whether the flame is above or below the moving point average.

- Keep a tally of the number of times the flame switches from being above or below the average.

- Divide the number of frames being analysed by the number of times the flame switches from being above or below the moving point average. This should represent the flame pulsation frequency.

5.4 Furniture Fire Pulsation Frequency Results

Results of this method for the furniture fires 'Chair 15' and 'Chair 16' are shown in Table 5-1.

Table 5-1 – Results of Flame Pulsation Frequency Analysis

Experiment	First Image Projected	Second Image Projected	Period of Moving Average	Pulsation Frequency (Hz)
Chair 15	Front View	Front View	1 second (25 frames)	8.50
			2 seconds (50 frames)	8.36
			4 seconds (100 frames)	7.99
			5 seconds (250 frames)	7.43
Chair 16	Front View	Front View	1 second (25 frames)	12.2
			2 seconds (50 frames)	9.26
			4 seconds (100 frames)	8.91
			5 seconds (250 frames)	8.58
	Side View	Side View	25	10.1
	Front View	Side View	25	10.7

The following graph plots the flame pulsation frequency against the period of the moving point average flame height.

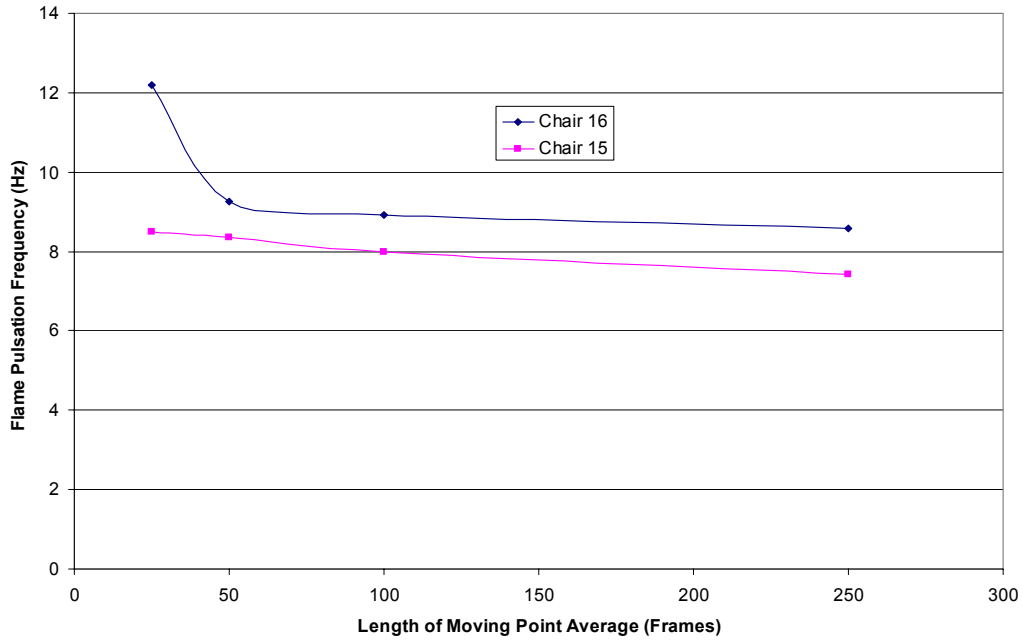

Figure 5-3 – Determined Flame Pulsation Frequency vs Period of Moving Point Average

5.5 0.8 m Poolfire Pulsation Frequency Results

As mentioned in the previous chapter, video of a 0.8 m poolfire was analysed to determine flame height, volume and pulsation frequency. Using the same techniques given for determining the pulsation frequency of the furniture fires in Section 5.3, the pulsation frequency was found to be 6.1 Hz. Using Equation (1) with the constant $\alpha = 1.50$, the pulsation frequency was estimated to be $f = 1.50/(0.8)^{1/2} = 1.7$ Hz and with $\alpha = 1.68$, $f = 1.9$ Hz.

5.6 Pulsation Frequency Discussion

The pulsation frequency found by analysing the flame heights of furniture fires was found to be between approximately 8 and 12 Hz when using a one-second average. For both furniture fire videos studied the flame pulsation frequency decreased as the period of the average increased. The values found were generally inside the range of 0.4 to 10 Hz for typical flame pulsation frequencies given by Cox (1995). However comparing the determined flame pulsation frequency to the estimated pulsation frequency using Equation (1) and a base diameter of 0.8 m shows that either the method used was incorrect, that Equation (1) is not applicable to furniture fires, or that the estimate of the base diameter was incorrect. Manually estimating the flame pulsation frequency from the original videos yields flame pulsation

frequencies of approximately 5 Hz and 6.5 Hz, respectively, which indicates that both possibilities are true.

When viewing the furniture fire videos frame by frame a phenomenon peculiar to these fires is observed. For periods of up to several seconds the flame alternates between peaking above either arm of the chair, with one peak ascending as the other is burning out. As the method for determining the flame pulsation frequency relies only on the maximum height of any part of the flame this leads to the pulsation frequency being overestimated. Therefore it is not possible to accurately determine the flame pulsation frequency of furniture fires from this method, nor is it possible to use a simple correlation such as Equation (1) to determine the flame pulsation frequency of non-pool fires.

Comparing the 0.8 m poolfire MRT result to the furniture fire result showed that different types of fires appear to produce different pulsation frequencies. At its peak, the furniture fires involved a similar base area to the poolfire, however the pulsation flame pulsation frequency for furniture fires can be between 2 and 5 times greater than pool fires. Any flame detection system that relies on determining pulsation frequency to initiate a warning or alarm phase should take into account the possibility that the pulsation frequency of an unwanted furniture fire may lie between approximately 0.4 and 12 Hz.

Chapter 6

Flame Volume Measurement

6.1 Introduction to Flame Volume

As stated earlier, it is thought that there exists a correlation between the volume of a flame and its heat release rate. However there has previously been no accurate method of determining the instantaneous volume of an uncontrolled diffusion flame to perform this comparison. This chapter outlines the method created to calculate the flame volume by using the minima reconstruction technique to convert video footage of furniture and pool fires into 3-dimensional representations.

Due to the unavailability of methods to determine flame volume, there is little on the subject in the literature. A correlation between flame volume and heat release rate is given by Rasbash et al., however the flame volumes used in this correlation were constructed out of a cone on top of a cylinder which is half to two thirds of the total flame height high. The derivation of Equation (10 a) has been presented elsewhere in this thesis:

$$\dot{Q} = 0.851V^{0.847} \tag{10a}$$

As mentioned earlier, Cox (1995) has estimated the heat release rate to be roughly 500 kW per m^3 of flame. This means there may be a rough relationship of the form:

$$Q = \gamma V \tag{19}$$

The coefficient γ will be found for the two furniture fires with the flame volumes calculated by determining the volume of the projected point cloud with a certain range of probabilities. By examining the discrepancies between the γ-values at each probability the best probability level to perform the MRT for flame volume and heat release rate calculations will be found.

6.2 Minima Reduction Technique for Determining Flame Volume

The Minima Reduction Technique is again used to 'project' two approximately orthogonal images of a burning item of furniture to create a 3-dimensional point cloud representing the

flame in the same was as for the flame height determination. However, instead of using single frames of the video footage, an average image is created from 6 seconds worth of video footage. The technique used for creating these averaged images was described in Section 3.2.7:

6.3 Flame Volume Results

6.3.1 Furniture Fire Volume Results

Four different levels of probability in the point clouds resulting from performing the MRT on two separate furniture fires were investigated, as the probability level to perform the MRT at for accurate volume results is not intuitively known. The first probability level contained all the points remaining in the point cloud after processing, and the others contained only the points with probability greater than 25%, 50% or 75 %.

The following figures contain the flame volume for 'Chair 15' and 'Chair 16', as well as the experimental heat release rate which is calculated from gas concentration, temperature and velocity measurements in the extract hood above the furniture using methods explained by Hill (2003) and Enright (2000). The flame volume consists of all the points in the projected point cloud having probabilities greater than either 0%, 25%, 50% or 75%. Four values were chosen because we are unsure which of the flame volumes will best represent the actual flame volume when it comes to finding a correlation between the flame volume and heat release rate. A scalar constant converts the flame volume into a heat release rate. This constant was found for each probability level by calculating the sum of squares of differences between the experimental and 'fitted' heat release rates. Excel's Solver Add-on was used to minimise the sum of squares of differences by changing the constant γ. Each probability level resulted in a different value for the constant between the two chairs.

Video footage of an insufficient number of experiments has been analysed here to give a result that could be used in practise, however applying the techniques to more footage of furniture fires could be used to give an better estimate for use when no other method exists of determining the heat release rate.

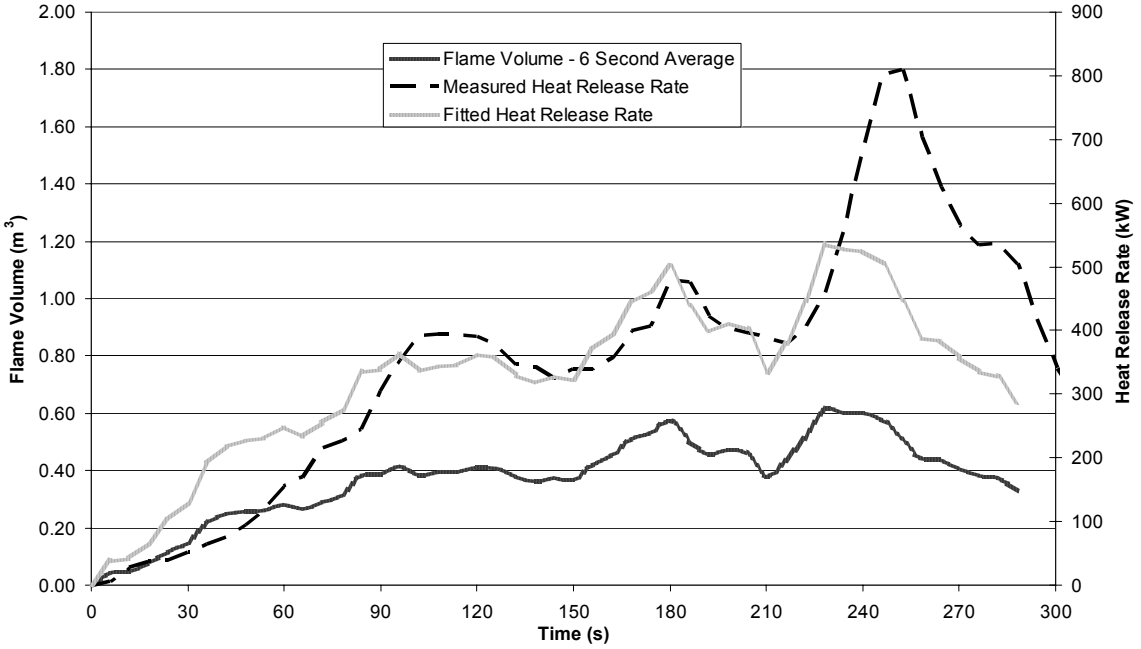

(a)

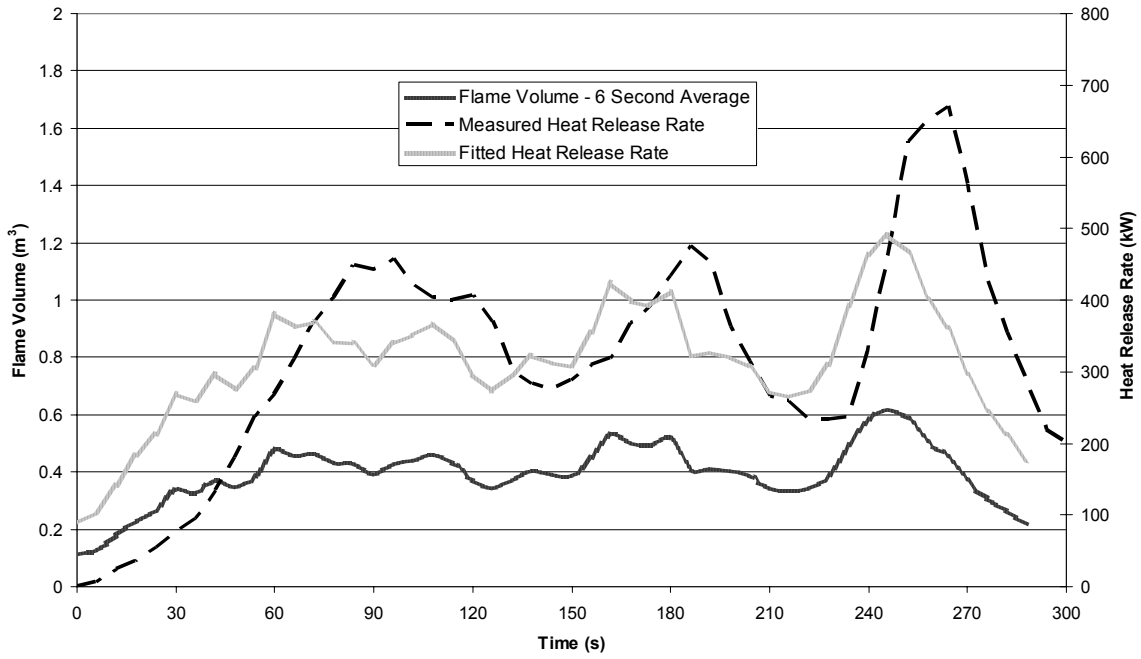

(b)

Figure 6-1 – Flame volume, heat release rate based on flame volume and experimental heat release rate for 'Chair 15' (a) and 'Chair 16' (b). Locations in the point cloud with probabilities in the range (0,1] were used. For (a) γ = 793 kW m^{-3} and for (b) γ = 873 kW m^{-3}.

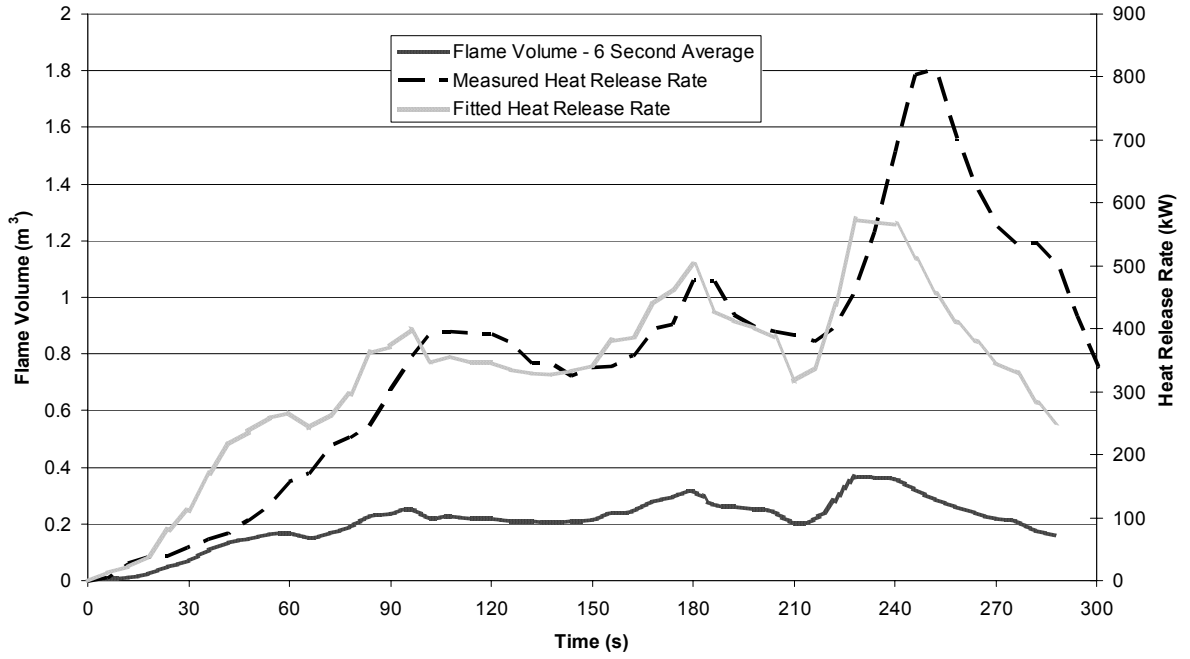

(a)

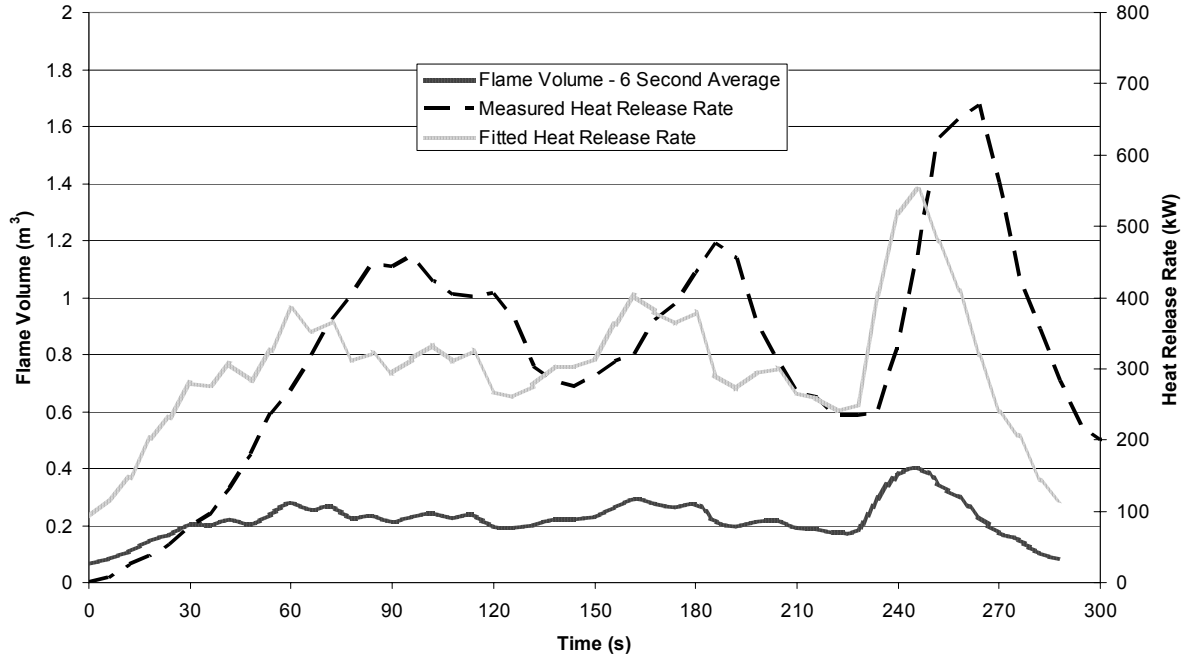

(b)

Figure 6-2 – Flame volume, heat release rate based on flame volume and experimental heat release rate for 'Chair 15' (a) and 'Chair 16' (b). Locations in the point cloud with probabilities in the range (0.25,1] were used. For (a) γ = 1570 kW m^{-3} and for (b) γ = 1361 kW m^{-3}.

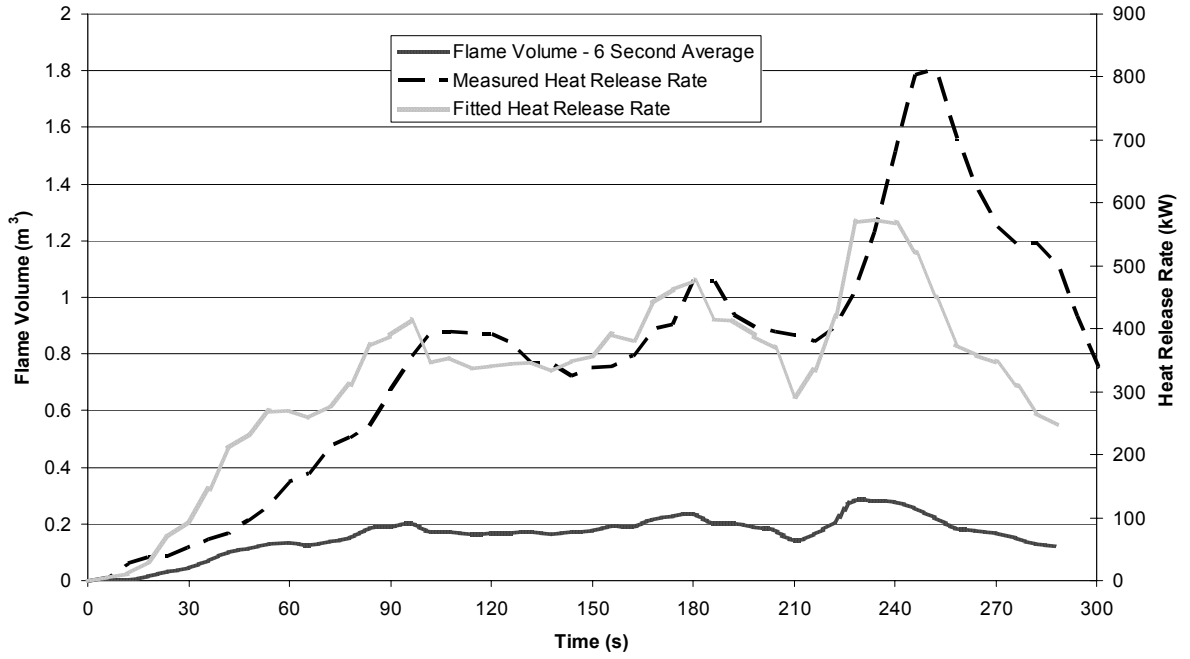

(a)

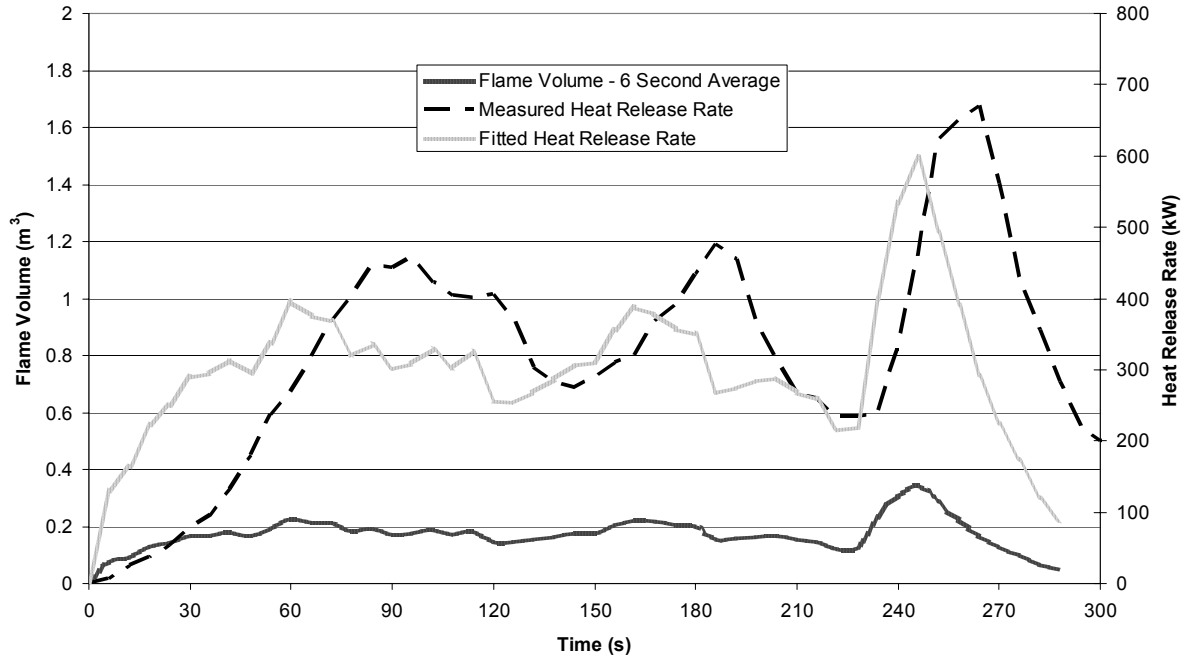

(b)

Figure 6-3 – Flame volume, heat release rate based on flame volume and experimental heat release rate for 'Chair 15' (a) and 'Chair 16' (b). Locations in the point cloud with probabilities in the range (0.5,1] were used. For (a) $\gamma = 2021$ kW m^{-3} and for (b) $\gamma = 1735$ kW m^{-3}.

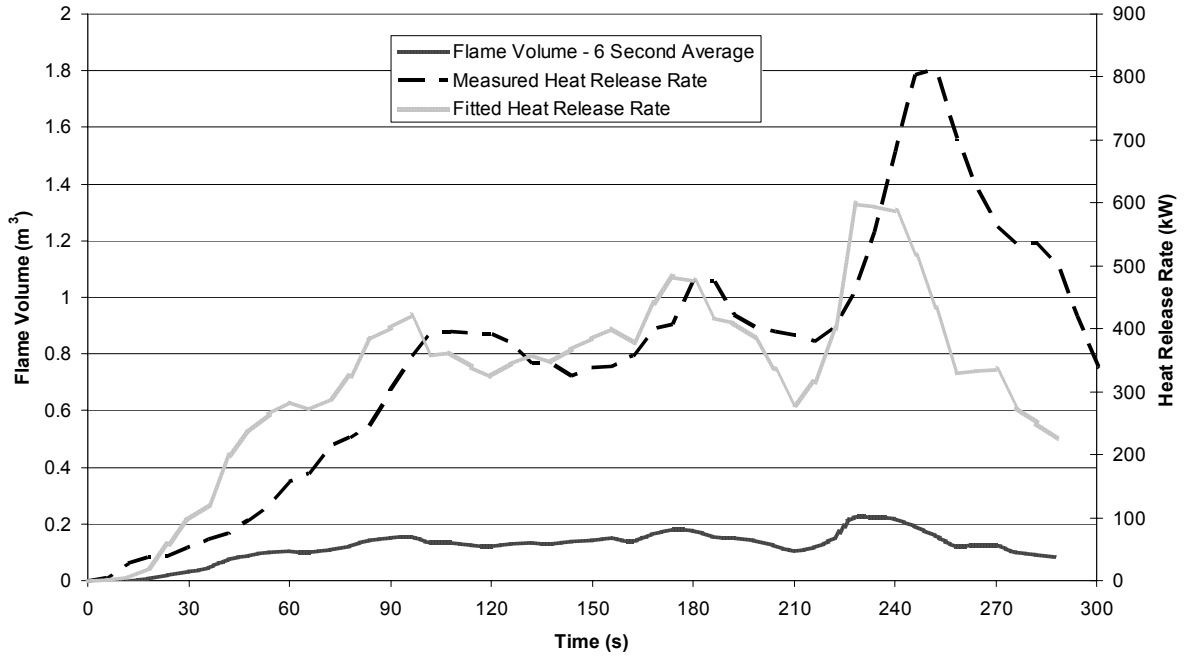

(a)

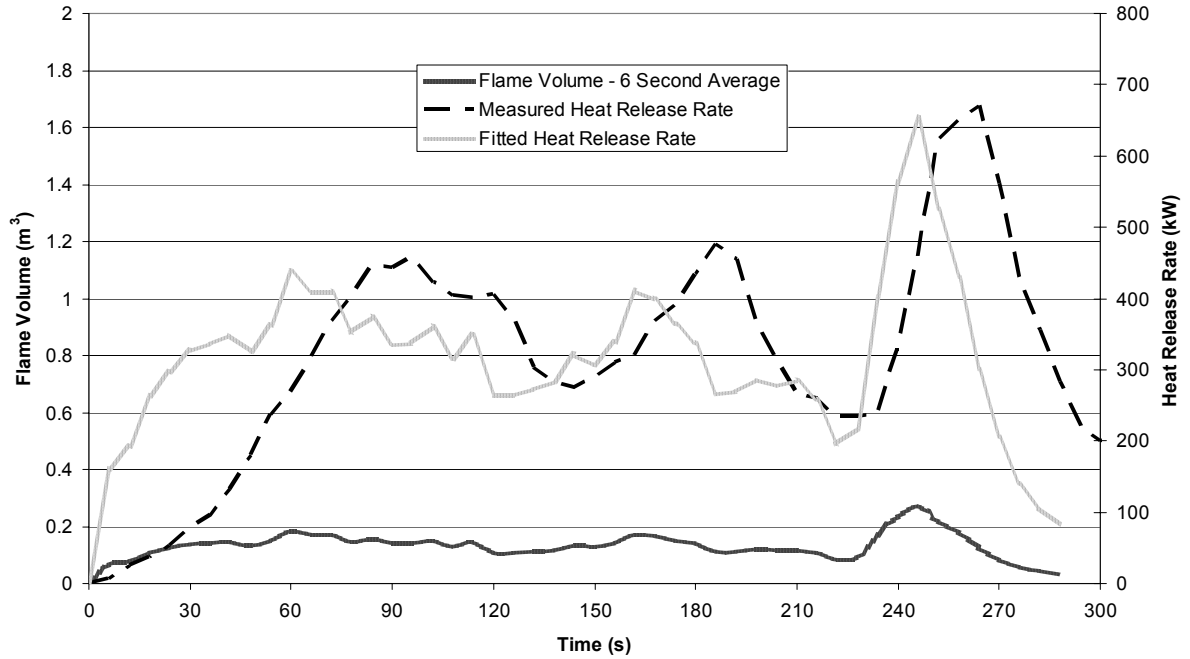

(b)

Figure 6-4 – Flame volume, heat release rate based on flame volume and experimental heat release rate for 'Chair 15' (a) and 'Chair 16' (b). Locations in the point cloud with probabilities in the range (0.75,1] were used. For (a) $\gamma = 2660$ kW m^{-3} and for (b) $\gamma = 2380$ kW m^{-3}.

Table 6-1 shows the γ-coefficients for Equation (18). The percentage difference was calculated as the difference between the two coefficients at each probability level, divided by the greater of the two.

Table 6-1 – Constants fitted to flame volumes to predict heat release rate and percentage discrepancy

Chair	γ_0	γ_{25}	γ_{50}	γ_{75}
15	873	1570	2021	2660
16	793	1362	1735	2380
% Difference	9%	13%	14%	11%

The results indicate that using all the points in the point cloud, rather than the 25%, 50% or 75% and higher probabilities, is the more accurate method of determining heat release rate from flame volume as there is less variability in the constant γ fitted to the data.

The Excel function LINEST was also used in an attempt to find a more accurate correlation than Equation (18), possibly similar to that given by Equation (10 a). LINEST is able to describe a linear trend between two sets of data as well as return regression statistics using a similar sum of squares method to that described above. LINEST returns the coefficients for the following form of equation:

$$y = a_1 * x_1 + a_1 * x_2 + ... + a_n x_n + b \tag{20}$$

Here, x_1, x_2 etc and y are variables, $a_1 \ldots a_n$ are gradients and b is the y-intercept. The x-variables can be functions of another variable, in this case, the volume. For this regression x-terms tried in LINEST included exponential and logarithmic terms (eg $V^{0.4}$, ln(V)). However none of the correlations found using LINEST were any more accurate than Equation (18), and they were certainly much more complex so the original correlation found was used.

6.3.2 Pool Fire Volume Results

Now that an estimate of the heat release rate per unit volume has been calculated, it can be applied to other fires. A series of methanol pool fires was carried out at the University of Canterbury in 2004. The diameter of the circular pans ranged from 0.10 to 0.80 m. The smaller fires did not provide sufficient contrast between the flame and a reflective panel on the door to the laboratory directly behind the flame. This would prevent our programs from

extracting an accurate representation of the flame. The 0.8 m diameter experiment was analysed using the techniques mentioned here to determine the flame volume throughout the experiment. The heat release rate is estimated using Equation (18) with $\gamma = 800$ kW m^{-3}:

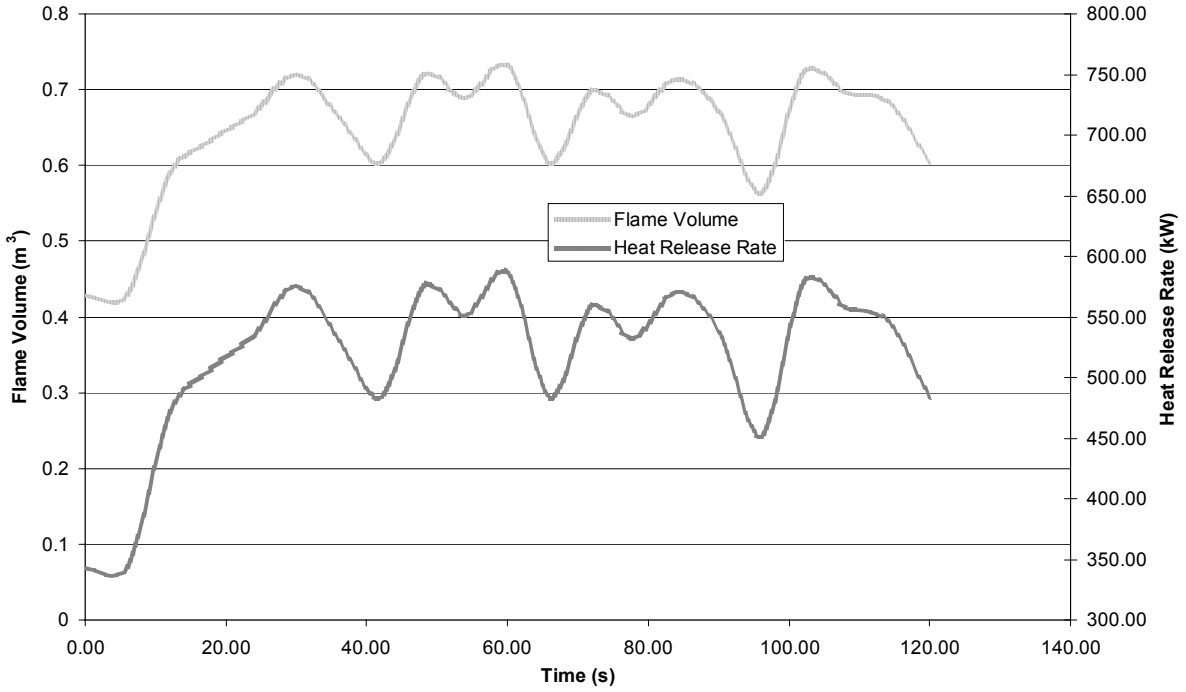

Figure 6-5 – 0.8 m poolfire volume and estimated heat release rate using $\gamma = 800$ kW m^{-3}

The heat release rate for the 0.8 m methanol diameter pool fire was previously estimated as 220 kW.

This indicates that our current estimation of the heat release rate using Equation (19) is inadequate for use with pool fires. One must bear in mind that the technique has only been applied to two furniture fires, and that more video footage should be analysed to find a more accurate constant γ. The discrepancy may also be due in part to incorrectly identifying the position of the camera in each of the furniture fire videos which led to a smaller volume, and hence a larger heat release rate per unit volume. As accurate measurements of the distances between the cameras and parts of the chair were not made during the experiments, this is another possible reason for discrepancies.

6.4 Another Method of Determining Flame Volume

Equation (10 a) from Rasbash shows there is a correlation between the heat release rate and flame volume. Although we could use the volume determined by the MRT method and apply

Equation (10 a) to get the heat release rate, in order to properly compare the two methods the volume should be calculated based on the flame height as proposed by Rasbash. The volume that was used in this correlation was estimated by assuming the flame was made up of a cylinder two thirds of the flame height with a cone on top of the cylinder. Since we have already determined the flame height during the experiments 'Chair 15' and 'Chair 16' for the previous chapters it is a simple matter to determine the flame volume based on an estimated diameter of the flame throughout the experiments. Therefore, assuming the flame base diameter is 0.8 m as we have throughout this analysis, the flame volume is calculated:

Volume of cylinder:

$$V = \frac{\pi}{4} D^2 z \tag{21}$$

$$V = \frac{\pi}{4} D^2 \left(\frac{2}{3} h_f \right)$$
$$V = \frac{3.14}{4} (0.8)^2 \left(\frac{2}{3} \right) h_f$$
$$V = 0.335 h_f$$

Volume of cone:

$$V = \frac{1}{3} \frac{\pi}{4} D^2 z \tag{22}$$

$$V = \frac{1}{3} \frac{\pi}{4} D^2 \left(\frac{1}{3} h_f \right)$$
$$V = \frac{1}{3} \frac{3.14}{4} 0.8^2 \left(\frac{1}{3} \right) h_f$$
$$V = 0.0558 h_f$$

Therefore, the total volume,

$$V = 0.391 h_f \tag{23}$$

Using the flame heights determined during the furniture fire experiments, the heat release rate can be approximated using Equation (10 a). For comparison, this heat release rate, the experimental heat release rate and the heat release rate estimated from the flame volume found using the MRT method are all shown in Figures 6-6 to 6-8 below:

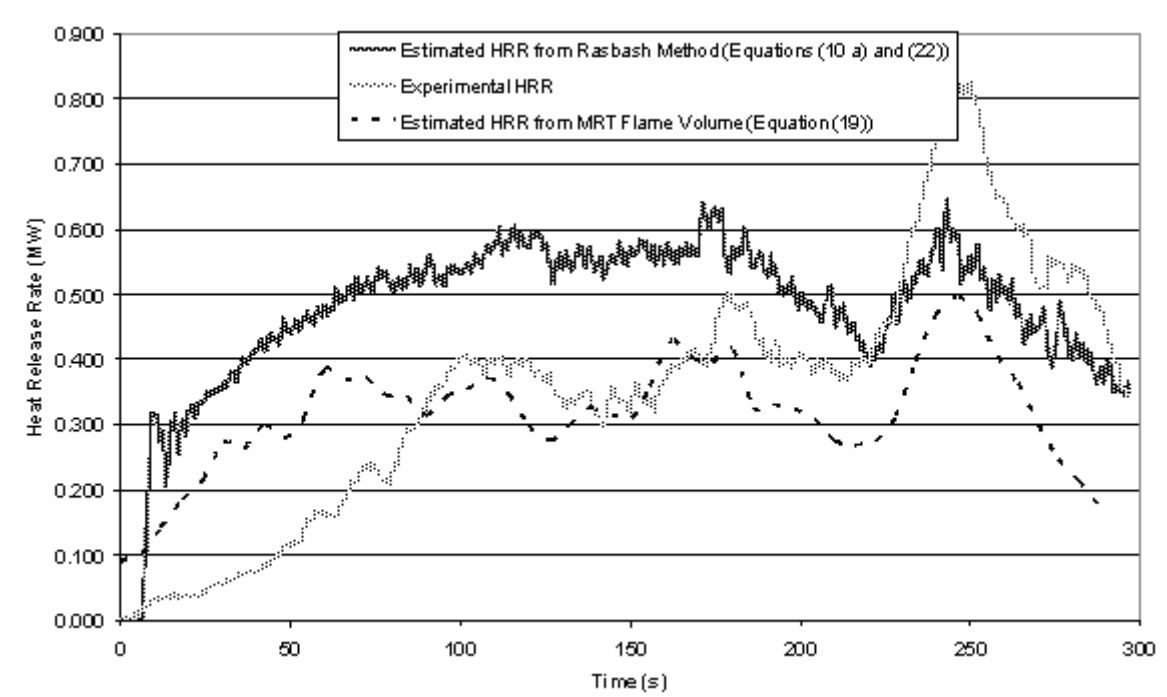

Figure 6-6 – 'Chair 15' heat release rate from experimental data, and estimated using simple (Equation (22)) volume with Equation (10 a) and MRT volume with Equation (18).

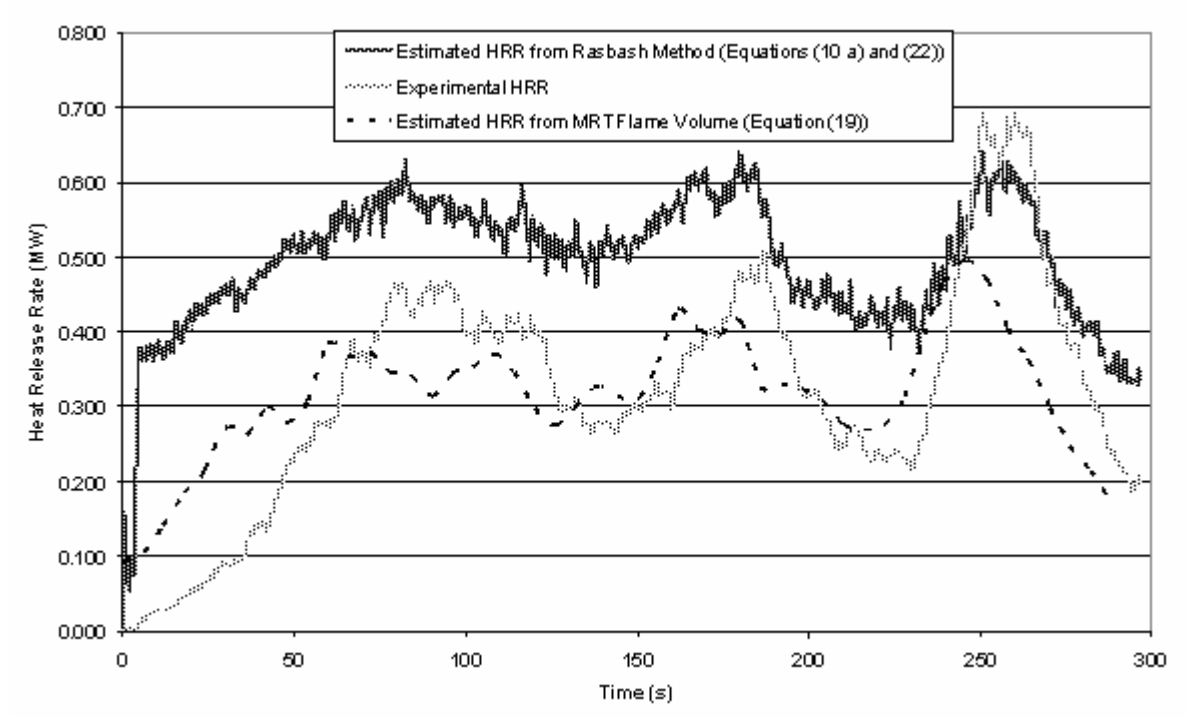

Figure 6-7 – 'Chair 16' heat release rate from experimental data, and estimated using simple (Equation (22)) volume with Equation (10 a) and MRT volume with Equation (18).

The same analysis was performed on the video of the 0.8 m poolfire analysed in Section 6.3.2. The volume of the flame is again determined using the MRT method and by using Equation

(22). The heat release rate is again calculated in the first instance by using Equation (10 a) and in the second using Equation (19). It is interesting to note that the volume and subsequently the heat release rate is more constant using this method proposed by Rasbash than the method proposed here.

6.5 Discussion of Flame Volume Results

The estimated constant in Equation (19) of roughly 800 kW m^{-3} is probably an improvement on the value given by Cox of 500 kW m^{-3}, however the correlation is tenuous at best and should only be used for rough estimates of the heat release rate when no other method is appropriate. There is obviously a significant error within this figure, as two non-identical furniture items burning gave disparate volumetric heat release rates of 873 and 793 for chairs 15 and 16 respectively. A 'round' figure of 800 kW m^{-3} is proposed as a rough estimate of the rate of heat release for furniture fires.

The fragile nature of the correlation can be shown by examining the experimental data from 'Chair 15'. In Figure 6-1 (a), the volume of the flame was determined to be close to 0.4 m^3 six times, however the heat release rate at each of these points was measured experimentally to range from approximately 280 to 800 kW.

The volume-heat release rate correlation overestimated the heat release rate during the growth stage of the furniture experiments and underestimated the heat release rate during the stages of peak heat release.

Applying Equation (19) and the methods developed for determining flame volume from video footage to non-furniture fires such as pool fires seems to overestimate the heat release rate. This may be due in part to the crude point cloud grid size which was used to estimate the flame volume for the entire pool fire experiment. The crude grid size was chosen because of the large amount of time each analysis takes to run, and the large increase in time per analysis that comes with reducing the grid size (see Section 3.4.1).

Estimating the volume of the flame as a combination of cylinder and cone volumes (Equation (22) led to a heat release rate from Equation (10 a) that was generally higher than both the experimental heat release rate and that derived using Equation (18) with γ = 800 kW m^{-3}. This indicates that our correlation, using the MRT method to determine the flame volume, is a more accurate method of estimating the heat release rate of furniture fires from video footage

than the method proposed by Rasbash. Concurrently, the radiative fraction of methanol is lower than that of the burning furniture, therefore the flame volume located by the video camera during the pool fire experiment would be lower than in the furniture fire experiments, and hence the estimated heat release rate is also lower than measured experimentally.

Figure 6-8 shows the comparison between the correlation found in this thesis and that implied by Rasbash and co-workers (Equation (10 a). The two are in surprisingly good agreement, considering the completely different ways the correlations were derived.

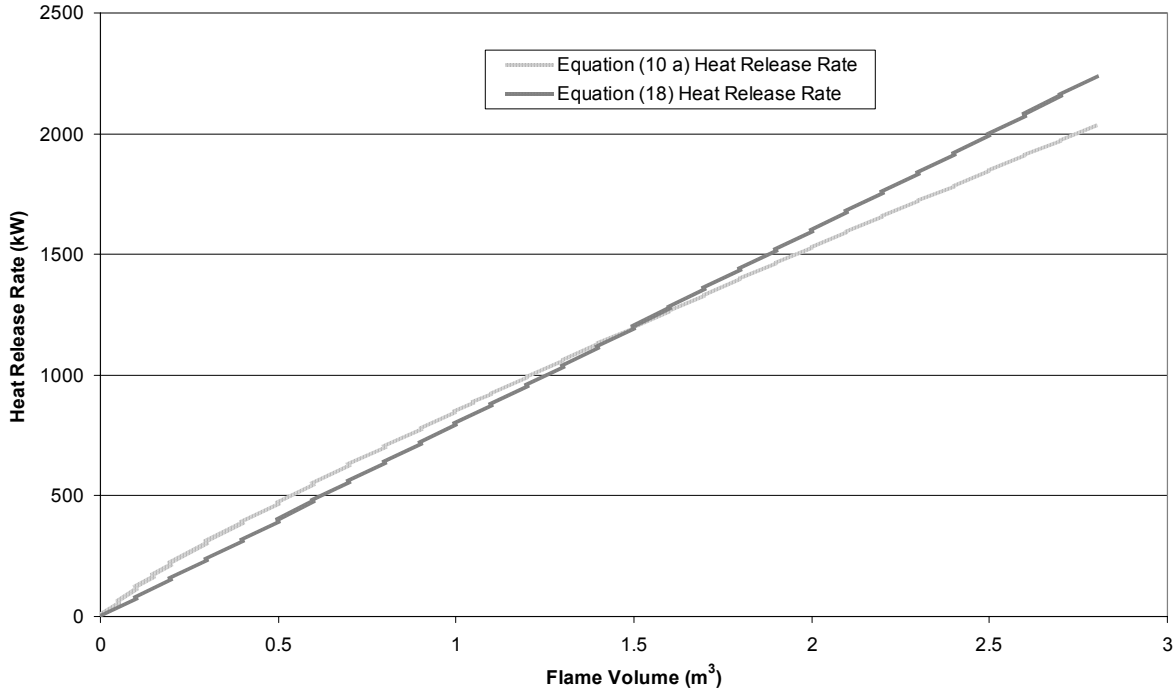

Figure 6-8 – Comparison between Equations (10 a) and (18) for converting between flame volume and heat release rate.

Using the method given by Rasbash et al. for determining the flame volume did not give as good agreement with the experimental heat release rate as using the MRT method did for either furniture experiment. Obviously, estimating the flame volume as a cylinder and cone combination will not accurately describe a fire with a shape as dynamic and unpredictable as a furniture fire. The comparison between the two methods when applied to the volumes found for 'Chair 15' and 'Chair 16' was shown in Figures 6-6 and 6-7. Calculating the sum of the squares of differences between the experimental and predicted heat release rates gives the 'goodness of fit'. Equation (19) gave rise to better heat release rate predictions than Equation (10a).

Chapter 7

Conclusions

7.1 Realisation of Aims

The methods given by Mason for developing a 3-dimensional representation of a flame which enables radiation shape factors to be determined. The aims of this research were to further develop these methods to enable the position of the flame tip to be located and calculate the flame volume from video footage. The flame volume was to be compared to the experimental heat release rate as measured by the furniture calorimeter to investigate the applicability of the figure given by Cox of 500 kW given off per m^3 of flame volume. A tentative value of 800 kW m^{-3} is given here based on the results of analysing only two videos of burning upholstered furniture.

This new figure of 800 kW m^{-3} was applied to the results of analysing video footage of a 0.8 m diameter pool fire, and compared to the heat release rate calculated for this fire of 94 kW. The volume of the flame was found to range from 0.43 to 0.73 m^3, which lead to an estimated heat release rate of between 380 and 660 kW.

It was found that the point cloud output given by Mason's programs allowed the flame volume and flame height to be determined easily. The most time-consuming part of the research involved changing his computer programs so that results for entire video files, and not just 6 seconds worth of flame data, could be processed with minimal user-interaction, and running the programs created for up to a week to analyse a single video.

7.2 Flame Height Conclusions

The minima reduction technique was able to locate the flame tip accurately in most cases. The flame height was determined by eye in 10 frames of the video file for 'Chair 16' and it was found that 8 of these were within 0.22 m of the determined flame height. This is a good result, as the accuracy of the MRT method was only ±0.11 m due to the fact that a uniform grid size was used in constructing the point cloud. Greater inaccuracies are likely to be due to the parameters used for manipulating each video frame (e.g. the threshold value or the colour plane extracted).

Figure 4-4 shows the effectiveness of the method compared to an estimate of the flame height which was based using the experimental heat release rate and assuming the flame diameter was 0.8 m. The base of the flame was always taken as the top of the seat cushion to avoid dealing with the problems associated with getting a computer program to recognise the true flame base. This means it is difficult to directly compare the flame height as determined by the MRT to that estimated using Equation (4). By assuming that the base of the flame would have moved closer and closer to the ground as the experiment progresses, the results of the two methods for estimating flame heights may be better resolved.

7.3 Flame Pulsation Frequency Conclusions

The flame pulsation frequency for two types of fire was found by examining the flame height data from Chapter 4. For all the fires examined, the pulsation frequency seemed to be quite high. Since no other methods for determining pulsation frequency were readily available (as they require highly priced photosensitive equipment), no comparison can be made.

Constants given by Cox and Malalasekera for Equation (1) were used to estimate the flame pulsation frequency for the three main fires considered. Both constants used grossly underestimated the pulsation frequency for the furniture and pool fires. The pulsation frequency for the furniture fires was predicted to be from 1.7-1.9 Hz, while the MRT method found the frequency to lie between 7.5 and 12 Hz. The prediction was slightly better for the pool fire examined, with the actual pulsation frequency here being approximately 6.1 Hz with the same estimate from Equation (1) of 1.7-1.9 Hz. The high pulsation frequencies are likely caused by deficiencies in both methods. Neither Equation (1) nor the MRT method are able to take into account the irregularities of a furniture fire flame such as the effects of the chair structure itself in creating multiple see-sawing flame tip positions simultaneously.

7.4 Flame Volume and Heat Release Rate Conclusions

The volume of two furniture fires was calculated using the MRT method. A constant of 800 kW m^{-3} was found for Equation (19), however further analysis of furniture fire videos would be required to give a more accurate figure.

Equation (19) was shown to predict very similar heat release rates compared to the slightly more complicated equation derived from Rasbash and co-workers' work (Equation (10 a)). The flame in their work was a cone and cylinder representation. The correlation was also

applied to a 0.8 m diameter pool fire. This fire was estimated to have a heat release rate of approximately 220 kW, however Equation (19) over-predicted the heat release rate of the pool fire by 2-3 times, indicating that Equation (19) may be unsuitable for application to non-furniture fires, or indeed there may be no further application of Equation (19) at all. Obviously it is difficult to make a direct comparison between the results, as the different fuels burnt (i.e. methanol vs polyurethane foam and wool/cotton fabric) makes it difficult to compare the results. Also, the heat release rate for the furniture items was measured with a fair degree of accuracy, whereas the pool fire heat release rate was only estimated using a correlation which makes any comparison difficult.

As mentioned earlier, Equation (19) coupled with the MRT method should only be applied when no other technique is available for determining the heat release rate.

7.5 Further Work

7.5.1 Further Laboratory Video Footage Analysis

Only two sets of furniture fire video footage was analysed, but there are many more sets of orthogonal video footage available at the University of Canterbury for further study. A more reliable constant γ for Equation (19) is the likely outcome of analysing more footage using the methods presented here.

Similarly, video footage of only one pool fire was analysed. A series of pool fires could be performed, with the heat release rate being determined using the furniture calorimeter. This would enable an accurate comparison between the flame volume from the MRT method described here and the heat release rate to determine the γ-value in Equation (19).

7.5.2 Field Video Footage Analysis

Video footage of field experiments can be shot and analysed using the methods described here, however these recommendations must be followed:

- The position of the camera relative to reference points in the frame must be located before the experiment begins. Tripods or similar mounting devices must be used for both cameras.

- The zoom function of the camera must not be used; it should remain at its widest setting.

- The entire flame must be captured by each camera. This means there should be sufficient distance between the camera and the flame before the experiment begins.

7.5.3 Sensitivity of MRT to Input Parameters

It has been noted in this thesis that the flame height and volume depend heavily on the input parameters when creating the greyscale/binary images. The sensitivity of short pieces of video footage to the following input parameters should be investigated; better guidance for setting these input parameters would be the likely result:

- **Colour plane extraction**. When examining future video footage, it is vital that the user experiment with all available colour planes to see how well the flame is located before running the MRT programs.

- **Threshold value**. Decreasing the threshold value would likely increase the average flame height located, bringing the MRT results more in line with those from the correlations given by McCaffrey and by Heskestad (Equation (4)). It is not known what effect this would have on the flame volume-heat release rate correlation.

7.5.4 Locating Base of Flame

It was stated in Section 4.6 that the base of the flame was assumed to be at the top of the seat cushion throughout the furniture fire experiments, however Figure 4-7 shows this is clearly not always the case. This Figure shows the difficulty involved in trying to get a computer program to identify the base of the flame. Further work could involve an algorithm to lower the base flame position as the heat release rate curve of the fire progresses. A simple example would involve setting the flame base as the top of the seat cushion for the beginning of the experiment, and at the floor level as the second peak in heat release rate starts to form due to the foam creating a pool beneath the chair and igniting.

7.5.5 Calculating Flame Surface Area

It was assumed throughout the volume analysis that the heat release rate depends proportionally to the volume of the flame. Since the visible flame is actually only a thin shell of reacting (combusting) material surrounding a volume of hot gases, it stands to reason that

the heat release rate may depend linearly on the surface area, since this quantity would better reflect the amount of combustion occurring. While using the radial basis function employed by Mason and described briefly in Section 3.4.2 would enable the surface area to be easily calculated, it should be possible to gain a rough estimate of the surface area using a program that joins the outer points in a point cloud and calculates the area of the surface created. For accuracy, this technique would require a finer grid resolution than was used in this thesis. The existence of a correlation between heat release rate and flame surface area could then be investigated.

Another possible method of determining the surface area of the flame would be to locate the outside of the flame in one image, and rotate this surface around the y (vertical) axis. The surface area could then be found using a numerical integration technique. This method would be better suited to axisymmetric flames and not furniture fires.

References

[1] Audouin, L., Kolb, G., Torero, J.L., Most, J.M., *Average Centreline Temperatures of a Buoyant Pool Fire Obtained by Image Processing of Video Recordings*, Fire Safety Journal, V 24, pp 167-187, 1995

[2] Barr, J., *Flames of Fuel Jets*, 4th Symposium (International) on Combustion, The Combustion Institute, pp 765-771, 1952

[3] Bejan, A., *Predicting the Pool Fire Vortex Shedding Frequency*, Journal of Heat Transfer, 113, pp 261-263, 1991

[4] Bhaduri, D., *Investigations on Pulsating Combustion*, Indian Journal of Technology, V 6, 1968

[5] Bradley, D., *How Fast Can We Burn*, Twenty-Fourth Symposium (International) on Combustion, The Combustion Institute, 1992, pp 247-262

[6] Carr, J.C., Beatson, R.K., Cherrie, J.B., Mitchell, T.J., Fright, W.R., McCallum, B.C., Evans, T.R., *Reconstruction and Representation of 3D Objects with Radial Basis Functions*, SIGGRAPH Proceedings, 2001

[7] Chamberlin, D.S., Rose, A., *The Flicker of Luminous Flames*, Industrial Engineering Chemistry, V 20, pp 1013-1016, 1928

[8] *Cortona* VRML client downloadable from: http://www.parallelgraphics.com/products/cortona/

[9] *Cosmo Player VRML Client* downloadable from: www.cai.com/cosmo/

[10] Coutin, M., Most, J.M., Delichatsios, M.A., Delichatsios, M.M., *Flame Heights in Wall Fires: Effects of Width, Confinement and Pyrolysis Length*, 6th IAFSS Proceedings, pp 729-740, 1999

[11] Cox, G. (Ed), *Combustion Fundamentals of Fire*, Academic Press, 1995

[12] Enright, P., *Heat Release and the Combustion Behaviour of Upholstered Furniture*, University of Canterbury, 2000

[13] Heskestad, G., *Fire Plumes, Flame Height and Air Entrainment*, SFPE Handbook of Fire Protection Engineering (3rd Edition), 2002.

[14] Heskestad, G., *Luminous Heights of Turbulent Diffusion Flames*, Fire Safety Journal, V5 pp 103-105, 1983.

[15] Heskestad, G., On *Q* and the Dynamics of Turbulent Diffusion Flames*, Fire Safety Journal, V 30, No 3, pp 215-227, 1997

[16] Hill, G.R., *Burning Behaviour of Upholstered Furniture*, University of Canterbury, 2003

[17] Huggett, C., *Estimation of the Rate of Heat Release by Means of Oxygen Consumption Measurements*, Fire and Materials, V 4, pp 61-65, 1980

[18] Karlsson, B. and Quintiere, J.G., *Enclosure Fire Dynamics*, CRC Press, 2000

[19] *Laser Doppler Anemometry - Principles*, http://www.dantecdynamics.com/LDA/Princip/Index.html

[20] Laskey, K.J., Zsak, T.W., Chigier, N., *Variations in Height of Laminar and Turbulent Flames*, Chemical and Physical Processes in Combustion, Combustion Institute, pp 4.1-4.4, 1984

[21] Malalasekera, W.M.G., Versteeg, H.K., Gilchrist, K., *A Review of Research and an Experimental Study on the Pulsation of Buoyant Diffusion Flames and Pool Fires*, Fire and Materials, V 20, pp 261-271, 1996

[22] Mason, P., *Estimating Thermal Radiation Fields from 3D Flame Reconstruction*, Lincoln University, 2003

[23] McCaffrey, B., *Flame Height*, SFPE Handbook of Fire Protection Engineering, 2nd Edition, National Fire Protection Association, Quincy, MA, 1995

[24] NT FIRE 032. *Upholstered Furniture: Burning Behaviour – Full-Scale Test*, Second Edition, 1991

[25] Pagni, P.J., *Some Unanswered Questions in Fluid Mechanics*, Appl. Mechanics Rev., 43, pp 153-170, 1990

[26] Puri, I.K., *Prediction of the Pulsation Frequency of Flames Formed Over a Semi-Infinite Horizontal Surface*, International Journal of Heat and Mass Transfer, V 36, No 10, pp 2657-2663, 1993

[27] Rad Video Tools, freely downloadable from "Rad Game Tools'" website http://www.radgametools.com

[28] Rasbash, D.J., Ramachandran, G., Kandola, B., *Evaluation of Fire Safety*, John Wiley and Sons, 2004

[29] Roberts, J.C., *Automatic Fire Detectors, Fire Protection Handbook*, 19th Edition, National Fire Protection Association, 2003

[30] Ruether, D., *On Video Image Characteristics and Faults*, http://www.ferrario.com/ruether/vid_pict_characts.htm, 2002

[31] Simard, A.J., Blank, R.W., Hobrla, S.L., *Measuring and Interpreting Flame Height in Wildland Fires*, Fire Technology, May, 1989

[32] Steward, F.R., *Linear Flame Heights for Various Fuels*, Combustion and Flame, V 8 pp 171-178, 1964

[33] Sugawa, O., Yasushi, O., Satoh, H., *Flame Height from Rectangular Fire Sources Considering Mixing Factor*, Proceedings 3rd International Symposium on Fire Safety Science, pp 435-444

[34] Thomas, P.H., Hinkley, P.L., Theobald, C.R., Simms, D.L., *Investigations into the Flow of Hot Gases in Roof Venting*, Fire Research Technical Paper No. 7, HMSO, London, 1963

[35] Young, I.T., Gerbrands, J.J., van Vliet, L.J., *Image Processing Fundamentals*: http://www.ph.tn.tudelft.nl/Courses/FIP/noframes/fip.html

[36] Zukoski, E.E., Cetegen, B.M., Kubota, T., *Visible Structure of Buoyant Diffusion Flames*, 20th Symposium on Combustion, Combustion Institute, Pittsburgh, PA, pp 361-366, 1984

Appendix A – Chair Characteristics

This information is taken from Hill, 2003.

Table A-1 – Upholstered Furniture Characteristics

	Chair 15	**Chair 16**
Foam Type	'Public Auditorium' Foam	'Domestic Furniture' Foam
Fabric Type	95% Wool, 5% Nylon	100% Cotton
Frame Material	*Pinus radiata* timber	*Pinus radiata* timber

The figure below shows the frame dimensions (in mm) of the two chairs analysed in this thesis. There were no struts between chair legs at the base. All other dimensions of foam and frame etc are 100 mm or multiples thereof.

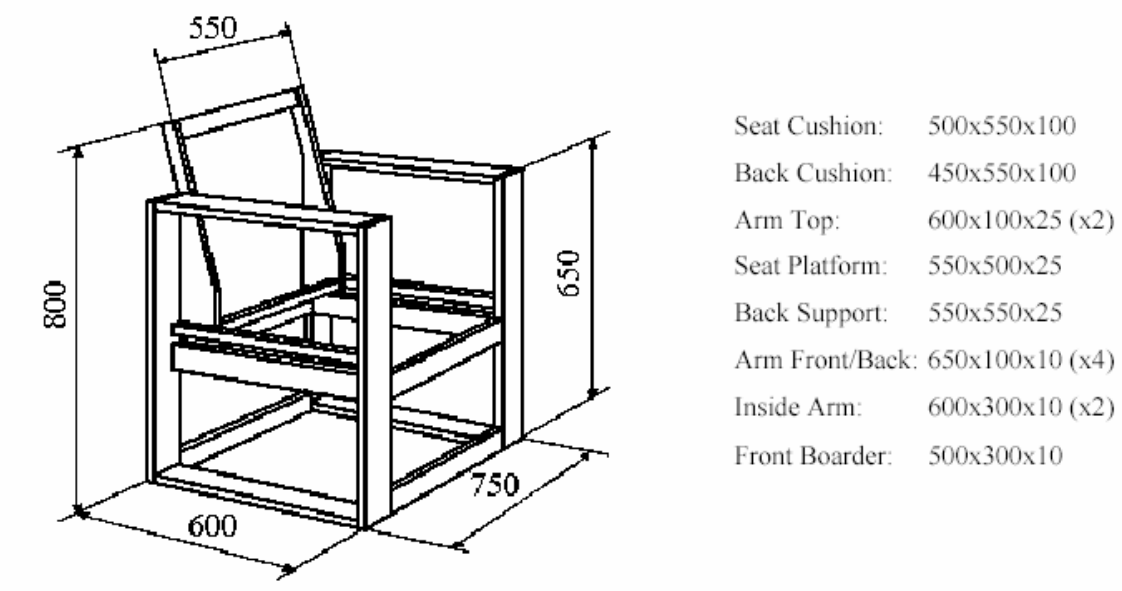

Figure A-7-1 – Frame and Foam Dimensions for Standard Chair Design (S1).

Appendix B – Use of LabVIEW Programs

The programs written for this thesis are available from the author or from the thesis supervisors on request. These are provided on an "as is" basis and no warranty of any kind is made to their use or applicability.

LabVIEW virtual instrumentation software is available from National Instruments Co.

The LabVIEW programs written for this thesis can be applied to video footage taken from multiple angles from multiple directions. An indication of the main inputs into the programs follows, along with an approximate indication of the time required to process each task (based on analysing 2*5-minute videos). The approximate computer processing time is based on using an AMD K2 500 MHz processor. Total user input time will be approximately half an hour for each analysis.

1. Extract .jpg images from the video files using a freely available program such as Rad Video Tools. (Time to process ≈ 2 hours).

2. Open the LabView Program:

   "CLocateRefPts Flame BJS.vi"

   Follow the instructions to find the screen coordinates of 2 reference points for an image from the first set of video files. Repeat for the second set of video files. (Time to process ≈ 2 minutes per file).

To Find Flame Height

3. Open the LabView program:

   "Averaging\Images2AverageBlairPulsation Average.vi"

This program will convert the colour .jpg files into binary .jpg files. Required inputs are:

   a. Path to directories containing colour images

   b. Upper and lower thresholding bounds

c. Colour plane to extract

d. Rotation angle

4. Open the LabView library:

   "Projection\CanterburyMRT.llb."

   When prompted, select the .vi:

   "CMRT_Main_Individual_Frames.vi"

5. Follow the instructions within the .vi. Inputs required are:

   a. Location of averaged images

   b. Path and filename to write output file into

   c. Screen coordinates of reference points (from step 4 above)

   d. Real world coordinates of reference points and camera position

(Time to process ≈ 1 minute per binary image or 5 days for a 5 minute, 7500 frame video).

6. The results are output into a .txt file at the location specified at step 5. This file can be opened as a tab-delimited file in Excel for further processing.

To Find Flame Volume

3. Open the LabView program:

   "Averaging\Images2Average 6 Second Average.vi"

   This program will average a specified number of colour .jpg files into averaged greyscale .jpg files. Required inputs are:

   a. Path to directories containing colour images

   b. Upper and lower thresholding bounds

   c. Colour plane to extract

d. Rotation angle

e. Number of images to average (150 = 6 seconds at 25 frames per second).

(Time to process ≈ 2 minutes per file).

4. Open the LabView library:

   "Projection\CanterburyMRT.llb."

   When prompted, select the .vi:

   "CMRT_Main_6_Second_Average.vi"

5. Follow the instructions within the .vi. Inputs required are:

   a. Location of averaged images

   b. Path and filename to write output file into

   c. Screen coordinates of reference points (from step 4 above)

   d. Real world coordinates of reference points and camera position

   Again, this step will take approximately 1 minute per greyscale file processed, however since there are fewer files to analyse, the time taken will be substantially lower.

6. The results are output into a .txt file at the location specified at step 5. This file can be opened as a tab-delimited file in Excel for further processing.

Using a similar computer to that used for this work, one should allow at least a day to analyse 5 minutes of video footage (at 6 frame averages) to determine flame volume, and one week to determine flame heights (at single frames) for the same length of video.